Mass spectrometric identification and quantification of mitochondrial proteins that are enriched or depleted in budding yeast lacking Tor1, a protein that accelerate chronological aging

Christine Abd El Malek

A Thesis

in

The Department

of Biology

Presented in Partial Fulfilment of the Requirements for the Degree of Master of Science (Biology) at Concordia University
Montreal, Quebec, Canada

August 2021

CONCORDIA UNIVERSITY
School of Graduate Studies

This is to certify that the thesis prepared

By: Christine Abd El Malek

Entitled: Mass spectrometric identification and quantification of mitochondrial proteins that are enriched or depleted in budding yeast lacking Tor1, a protein that accelerates chronological aging

and submitted in partial fulfillment of the requirements for the degree of

Master of Science (Biology)

complies with the regulations of the University and meets the accepted standards with respect to originality and quality.

Signed by the final Examining Committee:

_____Chair

Dr. Patrick Gulick

_____Examiner

Dr. Madoka Gray-Mitsumune

_____Examiner

Dr. Alisa Piekny

_____External Examiner

Dr. Elena Kuzmin

_____Supervisor

Dr. Vladimir Titorenko

Approved by_____

Dr. Robert Weladji, Graduate Program director

_____

Dr. Pascale Sicotte, Dean, Faculty of Arts and Science

Date _____

ABSTRACT

Mass spectrometric identification and quantification of mitochondrial proteins that are enriched or depleted in budding yeast lacking Tor1, a protein that accelerate chronological aging

Christine Abd El Malek, M.Sc.

The study of aging captured the interest of many researchers as the accumulation of old cells appeared to be linked to several chronic age-related diseases. Despite the complexity of the aging process, the pathways underlying cellular aging were revealed with the help of molecular analyses using the budding yeast *Saccharomyces cerevisiae*. This model is a unicellular eukaryote that is intensively used in aging research as its mechanisms are evolutionarily conserved across phyla. Our laboratory focused on one of those pathways, namely target of rapamycin type 1 (TOR1) signal transduction network that regulates cell growth in response to the availability of nutrients and growth factors. As such, the TOR1 signaling network activates several pro-aging processes and inhibits some anti-aging processes. Genetic, dietary, or pharmacological manipulations suppressing TOR1 activity have been shown to extend the lifespan. Thus, the single-gene deletion mutant *tor1Δ* has been used to investigate the mitochondrial proteome using non-caloric restriction. Mitochondrial functionality is vital as their decline is a hallmark of cellular aging in evolutionarily distant eukaryotes. Mitochondria synthesize the bulk of cellular ATP by harboring pathways that link the tricarboxylic acid cycle and oxidative phosphorylation. Mitochondrial fusion and fission are essential contributors to mitochondrial functionality maintenance because they regulate the age-related changes in mitochondria assembly and biogenesis. Mass spectrometry was used to identify and quantify the purified mitochondrial proteins from differently aged control wild-type and *tor1Δ* mutant strains of budding yeast that were upregulated or downregulated. These findings suggest that some of the mitochondrial proteins in the *tor1Δ* mutant strain are upregulated and could contribute to the mechanism that extends lifespan in yeast cells.

ACKNOWLEDGEMENTS

I am grateful to my supervisor, Dr. Vladimir Titorenko, for giving me the opportunity to work in his laboratory and for the learning experience that I gained with his guidance. I would like to express my gratitude to my committee members, Dr. Patrick Gulick, and Dr. Madoka Gray-Mitsumume, for their great support and valuable feedback throughout my graduate research. I would like to thank the Center for Biological Applications for Mass Spectrometry (CBAMS), especially Dr. Heng Jiang for his valuable assistance and expertise. I would like to thank my mentor Dr. Younes Medkour who guided my learning process in proteomics. I would also like to thank all the laboratory members of the Titorenko lab for their cooperation and support.

TABLE OF CONTENT

LIST OF FIGURES

LIST OF TABLES

Chapter 1: Introduction

1.1 An overview of biological aging in yeast and other eukaryotes.

The budding yeast, *Saccharomyces cerevisiae*, is a genetically tractable unicellular eukaryote that has a relatively short lifespan and can be subjected to advanced molecular analyses to identify signaling pathways involved in delaying aging through changes in some key nutrient-sensing pathways [3,4, 24]. A distinct set of vital cellular processes is stimulated during aging in all eukaryotes [2]. These cellular processes define the longevity of budding yeast and other eukaryotes and are called the hallmarks of aging [2]. These hallmarks of aging include genomic instability, telomere attrition, deregulation nutrient sensing, mitochondrial dysfunction, stem cell exhaustion, and cellular senescence [2]. A gradual progression of the cellular processes constituting the hallmarks of aging via a series of lifespan checkpoints is monitored by a team of master regulator proteins [3]. These master regulator proteins define the pace of establishing a pro- or anti-aging cellular pattern in eukaryotes [3].

Certain dietary regimens and natural pharmacological interventions, such as rapamycin, appeared to target a major pro-aging pathway in yeast known as the TOR (target of rapamycin) signaling pathway [4,5]. This pro-aging pathway is regulated by amino acid abundance, and the rapamycin-dependent inhibition of the TOR pathway extends the lifespan of yeast cells because it activates the autophagy process [4, 5]. The genomic instability is the hallmark of aging promoted by DNA replication errors and reactive oxygen species (ROS) accumulation [2]. Genomic stability is essential for maintaining the appropriate telomere length and ensuring the integrity of mitochondrial DNA to avoid premature aging syndromes [2]. The accumulation of DNA damage affects the telomere region in the chromosome that can cause pulmonary fibrosis and aplastic anemia [2]. A slowdown of aging can be achieved by preserving the stability and functionality of the cellular proteomes with the help of molecular chaperones of the heat shock protein family [2]. Therefore, the impairment of protein folding or the inability to degrade misfolded proteins accelerates the aging process in all eukaryotes [2]. Dietary restriction has been shown to extend the longevity of various eukaryotes by downregulating the insulin and insulin-like growth factor 1 (IIS or IGF-1) signaling pathway and protein kinase A (PKA) signaling pathway [2,4]. Downregulation of the PKA pathway in budding yeast stimulates the serine/threonine-protein kinase Rim15p, activating the stress-response transcription factor Gis1, an ortholog to DAF-16 in nematodes and FOXO in fruit flies [2,4]. The resulting activation of Gis1, DAF-16, and FOXO

extend the lifespan in all these organisms because it stimulates the oxidative stress protecting superoxide dismutase (SOD) in mitochondria and cytoplasm and promotes the cytoprotective process of autophagy [2,4].

All these findings provide evidence that mechanisms of aging and aging delay have been conserved during evolution. Therefore, some aging hallmarks, such as genomic instability, telomere attrition, alteration in proteolytic activity in the cell, mitochondrial dysfunction, deregulation in the nutrient-sensing system, and further interference in the pathway of intercellular communications, are improved through the deletion of genes such as TOR [2].

1.2 Replicative and chronological aging of budding yeast.

The aging of *S. cerevisiae* can be assayed in different ways such as chronological lifespan (CLS) or replicative lifespan (RLS) [5, 24]. Studies of some aspects of chronological aging in budding yeast generated deep insights into the cellular mechanism underlying longevity regulation in evolutionarily distant eukaryotic organisms [4]. These studies discovered a biomolecular network orchestrating the cell-autonomous mechanisms of chronological aging in *S. cerevisiae* and other eukaryotes [3]. The checkpoints of the aging process in budding yeast and dissected the roles of master regulator proteins in passing each of these checkpoints [3].

The RLS assay evaluates the maximum number of daughter cells a mother cell can produce by the asymmetric mitotic division before it becomes senescent [5]. Replicative aging in budding yeast mimics the aging of mitotically active mammalian cells, including lymphocytes [5]. RLS in budding yeast can be measured by physically removing and counting the total number of the daughter cells that are produced by the mother cell until reaching the senescent state [5]. Budding yeast's RLS is described as a progression of *S. cerevisiae* through several functional states before entering a state of senescence [24]. Replicative aging in budding yeast results in the accumulation of the extrachromosomal ribosomal DNA circles (ERCs) in mother cells [24]. The ERCs are formed by homologous recombination within ribosomal DNA (rDNA) that stimulates an age-related accumulation of oxidative macromolecular damage, misfolding of cytoplasmic proteins, the buildup of dysfunctional mitochondria [24]. It ultimately accelerates cell entry into senescence to shortens its RLS [24]. Therefore, budding yeast's RLS studies are expected to discover the genes whose protein products control many aspects of replicative aging and are regulated by various chemical compounds from natural sources [24]. The second method used to quantify aging in yeast

cells is referred to as the chronological lifespan. The CLS assay measures the length of time during which a budding yeast cell remains viable (*i.e.*, being able to form a colony of cells on the surface of a solid medium) after an arrest of its growth and division [24]. Chronological aging in budding yeast mimics the aging of post-mitotic mammalian cells, including neurons [24]. Caloric restriction (CR) extends yeast CLS by suppressing both the TOR and insulin signaling pathways and activating the process of autophagy [24]. The early life checkpoints exist in the logarithmic (L), diauxic (D), and post diauxic (PD) phases of cell culturing, whereas the late-life checkpoint occurs in the stationary phase (ST) of cell culturing [21]. Under non-CR conditions (that are attributed by culturing yeast on 2% glucose as a carbon source), budding cells ferment glucose to ethanol and enter the PD phase of culturing as soon as glucose is consumed by cells [24]. At that point, budding yeast cells exit the cell cycle and enter a state of cellular quiescence [24]. The fermentation-dependent depletion of glucose produces ethanol, which is then metabolized to acetic acid to increase the cellular pH [24]. The increase in the cellular pH can elevate the toxicity in yeast cells because it induces ROS (reactive oxygen species) that causes oxidative damage to proteins [24]. The natural chemical compound can enhance the survival of yeast cells by reducing ROS toxicity in the cells [24].

The mitochondrial function is important for both the RLS and CLS. Proper mitochondrial segregation prevents mitochondrial proteotoxic stress and maintains proper nuclear mitochondrial communication by activating mitochondrial retrograde (RTG) signal pathways that are the crucial regulator for the RLS [20,21]. In addition, the daughter cells can eliminate ROS through asymmetrical protein inheritance [20]. The RTG signal decreases the mitochondrial membrane potential and transcribes genes that prevent mitochondrial dysfunction through reconfiguring metabolism by slowing down the synthesis of extrachromosomal rDNA circles [20,21]. Replicative aging slows down the aging process by activating Rtg2 and inhibiting TOR [21]. RTG signal supplies acetyl-CoA and citrate into the mitochondria to prevent TCA cycle disruption in yeast cells [20]. It was found that Afo1 reduction in mitochondria of RLS will cause activation in the anti-aging pathway allowing Spf1 protein to stimulate transcription of nuclear genes and inhibition of TOR signaling pathway [21].

On the other hand, inhibition of Sir2 protein will synthesize extrachromosomal rDNA circles, and activation of PKA will decline the anti-aging process of autophagy and stress response [21]. Therefore, activation of the RTG pathway extends the RLS and vacuolar acidification

decreases RLS [20]. CR and overexpression of *HAP4* were shown to extend RLS by enhancing mitochondrial respiration under a low level of glucose [20]. In addition, *HAP4* increases the NAD/NADH ratio, reducing the toxic rDNA circles and inhibiting the TOR pathway [20]. The CLS aging yeast cells also required mitochondrial respiration when the glucose is consumed, and there is a shift from fermentation to respiration (diauxic shift) [20]. Yeast cells have respiratory reserve capacity to sustain CLS to respire above the threshold [20]. However, respiration below the threshold during growth reduces the respiratory capacity of the stationary wild-type cells [20]. In early life checkpoint 1, CR in yeast cells through having 0.5% glucose will extend CLS because it will inhibit TOR/SCH9 pathway, enhance stress-resistance mechanisms, increase respiration, and reduces the metabolic rate in the stationary phase for the slow consumption of stored nutrients [20,21]. Deleting *tor1* or *sch9* mimics the CR with similar mechanisms on CLS via increasing mitochondrial respiration, metabolic remodeling and induces autophagy [20]. In lifespan checkpoint 2 at the diauxic and post-diauxic phases, the rate of coupled mitochondrial respiration in yeast cells progresses, thereby maintaining the cellular trehalose homeostasis [21]. In checkpoint 3, the rate of couple mitochondrial respiration maintains a balance between protein folding and misfolding [21]. Checkpoint 4 in D and PD increases the ROS production from mitochondria in young yeast cells stimulating Msn2/4 and Gis1 [21]. Checkpoint 5 releases amino acids that activate TOR, which will attenuate protein synthesis in mitochondria [21]. In the stationary phase, checkpoint 6 will fragment the tubular mitochondrial network limiting CLS through apoptosis [21]. The mitochondrial ability to generate ROS above the threshold leading to apoptosis causes dysfunction of mitochondria in checkpoint 7 [21].

1.3 Signaling network of longevity regulation in budding yeast and the effect of several plant extracts.

Several longevity pathways affect the budding yeast, such as NAD-dependent histone deacetylase family pathway of proteins known as Sirtuins [17]. Sir2 protein in yeast cells catalyzes the posttranslational modification of proteins, increasing the RLS of mother cells [7]. It was described that Sir2 promotes the asymmetric retention of damaged proteins within mother cells and increases genomic stability in rDNA [7]. Furthermore, a pharmacological sirtuins-activating compound (STAC) called resveratrol increased the replicative life span in yeast, worms, and flies [7]. The second pathway is the 5$^{'}$-AMP-activated protein kinase (AMPK) that regulates metabolic

pathways by changing the abundance of AMP and ATP through the glucose uptake and oxidation of fats. It was shown that AMP activates AMPK and ATP inhibits it to regulate the energy in the cells through a direct response to AMP/ATP ratio [7]. Several cellular stress such as starvation, impaired mitochondrial respiration, and hypoxia activate the AMPK that aid in improving the health span in several eukaryotic organisms [7,8]. The third pathway involves insulin-like growth factor (IGF-1), which regulates longevity as it determines the development, growth, and proliferation in the cell cycle by engaging with the IGF-1 receptor (IGF-1R) [7,8]. The IGF-1R activates the TOR pathway and the downregulation of IGF-1 increases the lifespan in yeast cells [7,8]. The TOR is a serine/threonine-protein kinase, promoting cell division in response to nutrient and growth factors [7,8]. The cell arrest which happens in the stationary phase is due to starvation for essential nutrients [7,8]. In the stationary phase, various genes are expressed to help survive without nutrients to activate autophagy [8]. Mammals have mTOR protein that contains mTOR1 complex and mTOR2 [7,8]. mTOR1 promotes global messenger RNA (mRNA) translation, represses autophagy, and modulates mitochondrial metabolism [7,8]. Sch9 integrates with the cell growth by functioning downstream of TOR1 [8]. The TOR1 activate its downstream Sch9 via phosphorylation in its c-terminal, which stimulates ribosome biosynthesis and inhibits Tap42 [8]. Therefore, genetic inhibition of TOR signaling pathways or targeting TOR with pharmacological intervention increased lifespan in yeast and other eukaryotic organisms [7].

Some plant extract from the findings support delay aging under non-caloric restrictions and include the root and rhizome of *Cimicifuga racemose* (PE4), the root of *Valeriana officinalis L* (PE5), the whole plant *Passiflora incarnate L.* (PE6), the leaf of *Ginkgo biloba* (PE8), the seed of *Apium graveolens L.* (PE12) and the bark of *Salix Alba* (PE21) [6]. The effect of each plant extract on yeast cells was described using glucose as a carbon source producing ethanol in the process and when the glucose becomes depleted in the cells, they switch from fermentation to respiration to use ethanol, known as diauxic shift [8]. During the post-diauxic and stationary growth phases, these cells will express environmental stress response genes such as Rim15 that enter the nucleus and stimulates Msn2, Msn4, and Gis1 [8,17,19]. It has been shown that the upregulation of Msn2/4 transcription factors extends chronological lifespan via the inhibition of TOR [17,19]. Therefore, during the stationary phase, the ROS detoxification extends the CLS [19]. The six plant extracts could stimulate mitochondrial respiration, postpone age-dependent rise in protein oxidation, and decrease mitochondrial-generated ROS (reactive oxygen species), thus eliciting a hormetic

response [6]. The six-novel aging-delaying plant extracts were able to delay aging either by inhibiting pro-aging pathways, such as the TOR1, PKA, and Pkb-activating kinase homolog (PKH1/2), or by activating the anti-aging pathways such as Rim15p and SNF1 [6]. PE6 was able to extend the life span of budding yeast, but the mechanism is not well understood [6]. PE8 attenuates the effect of pro-aging PKA pathway inhibition on the anti-aging SNF1 kinase pathway [6]. PE4 prevents the inhibitory effect of the TOR1 pathway on the anti-aging SNF1 kinase pathway [6]. The TOR1 and PKH1/2 pro-aging pathways activate Sch9 via phosphorylation [6,8]. Sch9 is an indirect effector of sphingolipid signaling that inhibits the formation of autophagosomes in the cytosol [6,8]. In addition, PE5 does not allow the inhibition of the pro-aging PKA signaling pathway on an anti-aging Rim15p kinase, thus activating stress-response transcription factors to express the stress-protective genes that extend the CLS [6]. PE12 activates an anti-aging protein kinase Rim15, promoting stress protection and inhibiting the protein kinase PKH1/2-dependent phosphorylation of Sch9 by PE21 [6]. Thus, Sch9 inhibition allows Rim15p to translocate into the nucleus, where it stimulates the stress response transcriptional activator Gis1p [8]. In summary, gene deletion or plant extract regulate a different element of the aging network, thus eliciting a different effect on cell response to stress, protein synthesis, and autophagy in *Saccharomyces cerevisiae* [6].

1.4 The protein kinase Tor1 is a central negative regulator of longevity in budding yeast and other eukaryotes.

The research on the target of rapamycin (Tor) originated in the 1960s to identify products from plants and soil [11]. Suren Sehgal identified rapamycin, a small molecule with anti-fungal activity from a soil bacterium called *Streptomyces hygroscopius* [11]. Tor is a target of rapamycin that can directly be bounded and has the potential to delay the S-phase entry to G1 cell cycle progression as the TOR activity is strongly associated with various human cancers [10,11,12]. Therefore, it shows that hyperactivity of TOR triggers ectopic cell proliferation under some circumstances [12]. At the molecular level, both Tor1p and Tor2p assemble into protein kinase TORC1 and were first identified in yeast cells and other eukaryotes [9,10,19]. On the other hand, TORC2 only contains Tor2p [19]. The Tor signaling pathway consists of a central signaling core composed of serine/threonine kinase Akt with a negative regulator such as Tsc1/Tsc2, PRAS40, and deptor [10,9]. Akt activates TOR1 by phosphorylating Tsc2 through binding of GTP to Rheb;

however, in unphosphorylated state of Tsc2 in complex with Tsc1 inhibits the activity of small GTPase Rheb [14]. Tuberous sclerosis complex 1 & 2 (Tsc1/Tsc2) inhibits the TOR activity, thus Akt phosphorylation inhibits Tsc2 resulting in TOR activation [12,13,14]. Tor1 is a central signaling core that integrates many signals from intra- and extracellular environments, influencing multiple responses for mRNA translation, autophagy, and mitochondrial oxidative phosphorylation [9,14]. The damaged cell starts to de-differentiate as the first step in repairing the cell through the inactivation of TOR and activating autophagy to clear up cellular content. Later, TOR reactivates for the cell cycle to re-enter proliferation [12].

In yeast, Torc1 has 2 major effectors, the AGC-family kinase Sch9, and Tap42, where the TORC1 executes its essential activities to promote protein synthesis through the gene encoding tRNAs, ribosomal proteins, ribosomal biogenesis factor and inhibits autophagy [10,13,17]. TOR directly phosphorylates sch9 modulating cytoplasmic translation and cell cycle progression, which are both negative regulators of chronological aging [18]. Deleting TOR1 has a similar effect to deleting sch9 that was suggested that it could be downstream of TOR-dependent mitochondrial regulation [18]. Current evidence across diverse taxa shows that TOR evolved to maintain cellular homeostasis, indicating that TOR is evolutionarily conserved [9,12]. The mTORC1 is sensitive to the availability of glucose that is regulated by AMPK [13,14]. When there is a drop in the cell's energy content by the rise of the AMP/ATP ratio, AMPK becomes active and suppresses TOR signaling core by phosphorylating Tsc2 [9]. Phosphorylating Tsc2 at a different site with distinct kinases results in either activation or inhibition of Tsc2's GAP activity such that Tsc2 is activated via AMPK phosphorylating, whereas Tsc2 is inhibited via Akt phosphorylation [14]. Mammalian TOR activity is sensitive to AMP/ATP likely sensed by pontin and Reptin ATPase complex that stabilizes the TOR complexes only when ATP levels are high [12]. In unicellular eukaryote cells sense the presence or absence of nutrients to control growth; however, multicellular organisms require intercellular communication by diffusible growth factors to modulate Tor1 activity through Akt [9]. It was found that the activation of Wnt receptors inhibits glycogen synthase kinase 3 (Gsk3) that phosphorylates and activates Tsc2 by an AMPK phosphorylation that results in the inhibition of Tor [9,14]. The Tor1 responds to hypoxia, in which a low oxygen level stabilizes HIF1-α forming a heterodimer HIFα/ARNT activating hypoxic response genes that inhibit the tor1 by the activation of Tsc1/Tsc2 complex [9,14]. It was described that DR (dietary restrictions) extends the yeast chronological life span by diminishing the TOR activity; however, lowering the

glucose level did not further extend the lifespan of the tor1 deletion mutant [9]. DR is classically defined as a reduction of calorie intake without causing malnutrition and it shows to slow the progression of cancer and neurodegenerative diseases [9]. It was discovered in rodents that restricting amino acids such as tryptophan and methionine extended their life span by inhibiting the Tor activity with a noticeable reduction in body weight [9]. The Tor activity enhances translation initiation of mRNA by directly phosphorylating the eukaryotic initiation factor 4E-BP that acts as translational repressors and alleviates the repressive effects of 4E-BP [9,14]. The 4E-BPs represses the translation initiation factor by binding to the elF4E and blocking the association of eIF4E with eIF4G that showed in *C. elegans* an extension in life span via reducing the translation initiation [9,14]. On the other hand, Tor activity is enhanced via activation of S6 kinase (S6K) in mammal cells, an ortholog of sch9 kinase in yeast cells [14,18]. Human cells with mutations that hyperactivate the TOR drive excess ribosomal biogenesis because TOR activity is sensitive to nucleotides, mainly with rRNA [12,17]. This can cause hyperproduction of ribosomes without enough nucleotides to support the DNA replication during the S phase, leading to replication stress, DNA damage, and apoptosis [12]. When TOR activity is depleted, it slows the rate of ribosomal biogenesis such as loss of genes encoding the 60S ribosomal unit extends the lifespan of yeast cells due to the increase of respiration [9,12,14,17]. In human cells, multiple cues controlling TOR activity such as p53-Sestrin2-mTORC1 and GATOR1 were found to repress TOR [12]. The p53 is a transcription factor stabilized by multiple stresses including, DNA damage, ribosome biogenesis stress, and hypoxia [12]. Sestrin2 is a leucine sensor for TOR in humans in which leucine directly binds to Sestrin2; thus, disrupting the interaction between Sestrin2 and protein complex called GATOR2 that will be free to repress GATOR1 and ultimately activate TOR [12]. Sestrins are not conserved in yeast; however, leucyl tRNA synthetase (LeuRS) is the only leucine sensor for TOR in yeast cells that act as GTPase activating protein (GAP) for Rags that stimulate TOR [12,13]. The mTORC1 is recruited to the lysosome by the Rag family of small GTPases [13]. Therefore, deletion of the *TOR1* activity extends the lifespan in eukaryotes by reducing TORC1 signals that are not lethal because tor2p can partially cover the loss of Tor1p in TORC1 [18]. On the other hand, tor2p deletion that causes the dysfunction in TORC2 is lethal [18,19].

1.5 Mitochondria play essential roles in the chronological aging of budding yeast and other Eukaryotes.

Mitochondria is a maternal heredity found in the vast majority of eukaryotic organisms that plays a vital role in providing bioenergetic and biosynthetic pathways to adjust the metabolic needs of the cell [15,26]. In addition, mitochondria maintain homeostasis of macromolecules such as lipids, proteins, heme, and iron-sulfur clusters that are central to diverse biological outcomes to proliferate and differentiate [15,26]. Mitochondria has its unique DNA (mtDNA) that encodes mitochondrial genes for oxidative phosphorylation (OXPHOS) machinery and synthesizes protein to trace the evolutionary origin of mitochondria [15,17,26]. Mitochondria are dynamic organelles most likely originated from α-proteobacteria that provide ATP, hydrogen, carbon dioxide, and detoxify ROS (reactive oxygen species) for their endosymbiosis relationship with archaeon [26]. As the hydrogen and carbon dioxide became limiting in the environment, then the α-proteobacteria fused with their host archaeon by endocytosis due to the force attraction and that metabolic symbiosis evolved into the first eukaryotic cell with mitochondria (*i.e.* α-proteobacteria) [26]. However, mitochondria are abundant electron donors that can provide electrons to oxygen generating ROS leading to toxification more than detoxifying the oxygen [26]. Similar to the bacterial ancestor, mitochondria contain their genetic machinery and consist of two functional distinct outer mitochondrial membranes (OMM), serves as a scaffold for signaling complexes and control of cell death, and inner mitochondrial membrane (IMM) that encapsulate the intermembrane space (IMS) and matrix compartment [15].

Mitochondria are known to be the powerhouse of the eukaryotic cells because it synthesizes the most cellular ATP through the tricarboxylic acid (TCA) and oxidative phosphorylation (OXPHOS) [15]. Mitochondria are organized in a tubular network by opposing fission and fusion processes to meet the cell's metabolic requirements [15,25]. Fission results in numerous mitochondrial fragments; however, fusion results in interconnected mitochondria to share efficient mixing enzymes, metabolites, or gene products [15,25]. Mitochondrial cristae increase the IMM's surface area to allow efficient processes such as OXPHOS with a high curvature membrane for the ATP synthase complexes in dimer joined at an angle [25]. The TCA cycle is carried in the matrix with eight enzymes linked to carbohydrates, fats, and proteins generating acetyl CoA with electron donors through the NADH and FADH [25]. Mitochondrial genome size and content is highly diverse between eukaryotes, as in *S. cerevisiae* mitochondrial genes represent 15% of the total

cellular DNA encoding for eight major subunit proteins that are complex III (Cytb), IV (Cox1, Cox2, Cox3), and V (Atp6, Atp8, and Atp9) responsible for electron transport chain and OXPHOS; in addition to one ribosomal protein of the small subunit (Var1) [15]. The OXPHOS synthesizes ATP through a large protein complex embedded in the IMM [25]. In yeast, it was described that the transfer of genes from mitochondrial genes to the nucleus is the favored direction [15]. Mitochondrial proteome isolated ~851 unique proteins in yeast using LC-MS mass-spectrometric method [15]. It is known that mitochondrial genetic machinery is responsible for the transcription and translation of the mitochondrial genome [15]. Mitochondrial proteins are synthesized in the cytosol and directed to their specific location by targeting signals [15]. Proteins are imported through a pre-sequence pathway in translocase of the outer membrane through pores in the TOM complex [15]. This is recognized by receptors of the inner membrane 23 (TIM23) driven electrophoretically via membrane potential of IMM [15]. Other protein translocases in the matrix are driven by a pre-sequence-associated motor (PAM) through ATP hydrolyzing HSP70 (Ssc1) subunit [5]. Most metabolites carriers and hydrophobic IMM proteins are synthesized containing multiple targeting signals within the sequence of the mature proteins translocated through TOM bound by Tim9-Tim10 & Tim8-Tim13 chaperone complexes inside the IMS. These proteins are delivered to the TIM22 translocase complex of the IMM [15,25]. The IMS protein import and assemble (MIA) machinery responsible for disulfide bond formation consist of Mia40 and Erv1 [15]. The preprotein is translocated through TOM and binds to Mia40 for oxidoreductase introducing disulfide bonds into the imported proteins to be stably folded [15]. This allows the electron transfer from oxidizing imported protein Erv1 to the molecular oxygen via cytochrome c [15].

During the CR, the Ras/cAMP/PKA promotes stress resistance transcription factors such as SOD2 [20,25]. Mitochondria generate ROS by-product of aerobic metabolism due to electrons leaking from their carrier systems, including superoxide and hydroxyl radical mediating toxicity because they are very reactive compared to molecular oxygen, which often leads to oxidative stress [15,23]. ROS is linked with the regulation of the chronological lifespan and apoptosis [15,23,25]. In yeast, the electron leakage in the respiratory chain could be found mainly in complex III than complex II and IV that are released in the IMS and matrix [15,23,25]. It was shown that superoxide dismutase (Sod1 and Sod2) converts superoxide to hydrogen peroxide to ensure that superoxide is maintained at a low concentration [15,25]. Sod1 is copper-zinc superoxide dismutase located in

IMS; however, Sod2 is a manganese superoxide dismutase localized in the mitochondrial matrix [15,25]. Hydrogen peroxide is not radical, but it can react with ferrous ion (Fe^{2+}) to form Fe^{3+} damaging proteins and genomic stability [15,25]. For that matter, yeast cell avoids forming Fe^{3+} by five enzymatic response such as peroxiredoxins (Tsa1, Tsa1, Ahp1, Dot5, and Prx1) and three glutathione peroxidases (Gpx1, Gpx2, and Gpx3) by converting H_2O_2 to water [15]. NADPH donates an electron to thioredoxin and glutathione reductase TRR and GTR that extends CLS under CR as they protect thiol-containing proteins from oxidative damage in mitochondria [23]. CR has a similar effect to natural pharmacological interventions such as rapamycin that inhibits TOR, leading to the increase of density of OXPHOS complexes and increase coupled respiration extending CLS [20,21]. CR activates PGC1-alph and improve mitochondrial function through antioxidant defenses, thus extending the longevity of budding yeast [20,21,23,25]. Mitochondria exchange metabolites between cytosol and mitochondrial matrix through the OMM, allowing molecules to transfer up to 4-5 kDa and IMM that is highly impermeable that allows small uncharged molecules to diffuse freely to the membrane [15]. Mitochondria include biogenesis of iron-sulfur (Fe/S) clusters that are cofactors with many vital functions such as catalytic sites, electron transfer, and sensory [15]. Mrs3/4 of the IMM imports iron by proton motive force synthesizing Fe/S on Isu1 scaffold protein that will interact with desulfurase complex of Nfs1, Isd11, and Acp1 [15]. This will release sulfur from cysteine to form alanine and persulfide that involve in the electron transfer chain comprising of ferredoxin reductase (Arh1) and ferredoxin (Yah1) [15]. Mitochondrial acyl carrier protein (Acp1) was shown to stabilize the complex and play a role in fatty acid metabolism [15]. The maturation of the Fe/S cluster requires a chaperone system consisting of Hsp70, ssq1, Jac1, nucleotide exchanging factor (Mge1), and monothiol glutaredoxin (Grx5) [15]. The Mge1 stimulates ATP hydrolysis activity of ssq1 allowing Jac1 to bind to Isu1, causing a conformational change, and allowing Isu1 and Grx5 to release the Fe/S cluster from Isu1 [15]. The depletion in Grx5 leads to accumulation of Fe/S cluster on Isu1 as the Grx5 acts as a transfer protein mediating the transfer of Fe/S clusters from Isu1 to apoproteins forming 2Fe-2S and 4Fe-4S required for specializing protein Isa1, Isa2, and Iba57 with unknown mechanism [15]. Depletion of those three proteins can lead to deficiency in cluster assembly on protein aconitase (Aco1) [15]. Heme is involved in sensing cellular oxygen levels by activation of transcription factor Hap1 that will regulate the oxygen responsive genes [15]. The membrane of the mitochondria is composed of phospholipids such as phosphatidylserine (PS),

phosphatidylinositol (PI), phosphatic cardiolipin (PA), and phospholipid cardiolipin (CL); however, the major ones are phosphatidylcholine (PC) and phosphatidylethanolamine (PE) that constitute 40% and 27% of the mitochondrial membrane respectively [15,23,22]. Synthesis of CL catalyzed by Cds1 detected in mitochondria and localized to the ER or Tam41 localized in the matrix side of IMM; in addition, it gets mature via Cld1 and Taz1[15]. In yeast and human cells, mitochondrial fatty acid synthesis (FAS) occurs in acyl carrier protein (ACP) that resemble bacterial type II FAS (mtFAS) that is needed for the synthesis of lipoic acid, which in turn is a cofactor essential for the function of pyruvate dehydrogenase (PDH) and alpha-ketoglutarate dehydrogenase [15]. The defects in mtFAS cause respiratory deficient phenotypes, resulting in a low level of lipoic acid [15]. A low level of lipoic acid could be due to a low level of glucose that will not produce enough pyruvate to convert into enough acetyl CoA going into mtFAD; therefore, decreasing the activity of PDH [15]. It was found that lithocholic bile acid (LCA) extends CLS by remolding mitochondrial lipidome [21]. The accumulation of triacylglycerol (TAGs) in lipid droplets (LD) extends CLS, and since the LCA is involved in the IMM and OMM through a bile acid that will modulate phospholipid synthesis dynamics in mitochondria [21,22]. LCA increases mitochondrial membrane phospholipid and improves mitochondrial functionality through proteome involved in ROS homeostasis, mitochondria respiration, and ATP synthesis [22].

1.6 Tor1 regulates some longevity-defining processes in mitochondria of yeast and other eukaryotes.

Mitochondria respiration is involved in age-related pathology as it is the major source of superoxide that can cause oxidative damage to mitochondria [19]. Around 40% of all genes involved in human diseases have an ortholog in yeast, and 70% of the nuclear genes are involved in mitochondrial disorders [15]. The critical point of mitochondrial protein translation is the mRNA translation initiation that is regulated by PI3K/Akt/mTORC1 with distinct mitochondrial ribosomes (mitoribosome), tRNAs, and translation factors than the cytosolic [16]. Some of the components of ETC complexes are encoded in the nuclear genome, translated into cytosolic ribosomes, and imported into the mitochondria via peptides that TOR regulates with the capacity of ATP production from the mitochondria [16].

The mTOR was associated with the outer mitochondrial membrane and treating with mitochondria with inhibitors results in TOR activity decrease [16]. The mitochondrial dynamics

are balanced between the fission and fusion processes [16]. The fusion process allows two different mitochondria to become one mitochondrion mediated by dynamin related GTPase such as MFN1, MFN2, and OPA1 to aid the cell stress by sharing multiple elements [16]. However, the mitochondrial fission divides one mitochondrion into two required for the segregation of damaged mitochondria for mitophagy, mtDNA replication, and mitochondrial redistribution [16]. In mammals exist 4 types of dynamin-related protein 1 (DRP1): mitochondrial fission 1 (FIS1), mitochondrial fission factor (MFF), mitochondrial dynamics protein 49 kDa (MID49), and MID51 located on the OMM [16]. It was described that mTOR is a regulator of mitochondrial dynamics and cell survival, as it promotes the mitochondrial translation proteins encoding mitochondrial fission process protein 1 (MTFP1) mediated by repressing 4E-BP [16]. Therefore, inhibiting the activity of mTOR phosphorylated DRP1 and prevents its translocation to mitochondria [16]. Mitochondria is regulated by mitochondrial biogenesis that allows the growth or division of pre-existing mitochondria and mitophagy is a form of autophagy that selectively degrades damaged mitochondria; therefore, they are two opposite processes [16]. Peroxisome proliferator-activated receptor-gamma co-factor 1-alpha (PGC1-alpha) and transcription co-activator are the master transcriptional regulators of mitochondrial biogenesis that bind to various TF and nuclear receptors promoting the mitochondrial biogenesis and oxidative phosphorylation in cancer cells [16]. PGC1 is a transcription factor for mitochondrial genes associated with yin-yang (YY1), which interact with the mTOR-raptor complex inducing the phosphorylation of YYT1 consequently favoring interaction PGC1-alpha, thus increase mitochondrial morphology and biogenesis state [16]. The mTOR1 controls mitochondrial biogenesis by selectively promoting the translation of mitochondrial mRNA via inhibition of 4E-BP, leading to the increase of ATP production [16]. It was shown that PGC1-beta and mTOR correlated with the mitochondrial activity found in breast cancer cells; therefore, knockdown of PGC-1beta decreased the mTOR expression [16]. On the other hand, the pro-mitophagy factor parkin was recruited to mitochondria with both genetic and chemical that induce loss of mitochondrial transmembrane potential to promote the mitophagy process [16]. Glutaminolysis is a reaction that occurs in the matrix and cytosol involving the degradation of the amino acid glutamine into glutamate, ammonium, aspartate, and pyruvate by glutaminase (GLS1 and GLS2 in mammals) that are important to replenish the TCA cycle by producing alpha-ketoglutarate (alpha-KG) via glutamate dehydrogenase (GDH) [16]. Glutamine is a non-essential amino acid except under hypoxic stress containing carbon and nitrogen in the

blood used to provide energy to the cell; glutamine participates in nucleic acid and protein synthesis [16]. Since the glutamine is mostly found in the plasma and muscle cells, cancer cells can generate energy from the glutaminolysis reaction that will result in the consumption of glutamine to satisfy nitrogen requirement in the cells leading to a loss in body's weight due to muscle mass consumption known as cachexia [16]. When mTOR activity is upregulated in several cancer cells, this increased cell growth and protein synthesis through the overexpression of glutaminase in the glutamine metabolism [16,23]. Therefore, inhibiting the GLS will lead to the deactivation of mTOR1 activity and increase autophagy and apoptosis [16,23]. It was shown that alpha-KG could be exported to the cytosol that can activate enzymes through a high glutaminolyc rate required for mTOR1 activation in HIF-1alpha independent manner to promote cell growth and inhibit autophagy [16]. A double-stranded DNA breaks sensor for serine/threonine-protein kinase ATM participating in cell cycle delay after DNA damage [16]. The glutaminolysis and mTORC1 act in both directions regulating each other to promote cell growth, in which glutaminolysis activate mTORC1 causing inhibition of autophagy and suppressing ATM via S6K1/2 signaling [16].

Oncometabolites refer to dominant mutations in the mitochondrial enzyme that are intermediates of mitochondrial metabolism and abnormally accumulate in cancer cells due to loss or gain of function [16,23]. It was shown that mTORC1 promotes the generation of oncometabolite [16]. In the TCA cycle, an enzyme Isocitrate dehydrogenase 1 and 2 (IDH1 and IDH2) catalyzes the oxidative decarboxylation of isocitrate to alpha-KG and producing NADPH [16,23]. Mutation in IDH1 and IDH2 genes by missense variants lead to substitution of arginine [16]. These mutations will gain the function of catalyzing alpha-KG to R-enantiomer of 2-hydroxyglutarate (2HG) that cause accumulation in cancer cells known as a biomarker for oncometabolite impairing hypoxic regulation [16]. The 2HG was shown to inhibit the alpha-KG that will affect the stability of DEPTOR, which is a negative regulator to mTORC1, causing the mTOR activation [16]. Therefore, rapamycin reduced the 2HG level in cells with mutant IDH via inhibiting mTORC1 activity [16]. In the TCA cycle, fumarate hydratase (FH) catalyzes the reversible hydration of fumarate to malate; in addition, FH has oncogenic properties that highly accumulate fumarate intracellularly [16]. The oncometabolite FH shares a similar structure to 2-oxoglutarate (2OG) that catalyze the hydroxylation with enzyme 2-OG dependent dioxygenases that belong to prolyl hydroxylases [16]. A high level of fumarate inhibits the HIF-alpha prolyl hydroxylases that will

stabilize HIF-alpha, a transcription factor promoting glycolysis in tumors [16]. Therefore, a global DNA methylation alteration is caused by high levels of fumarate and Succinate [16]. Moreover, it was shown that mTORC1 upregulation of fumarate accumulation develops cancer cells [16,17].

Wild-type yeast cells prefer glycolysis over respiration; therefore, they repress respiration in the presence of glucose as a carbon source [17]. It was shown in a previous study that mutating glucose-repression-defective (REG) will increase cell survival like deleting TOR1 since it shows an increase in respiration that is responsible for the extension of lifespan [17]. Yeast cells survive better when the TOR gene is deleted because it enhances mitochondrial respiration driven by an increasing number of OXPHOS complexes per organelle, increase oxygen consumption and decrease ROS production limiting the cellular damage components [18,19,23]. A balance between pumping proton determines mitochondria membrane potential through the electron transport chain and the dissipation of proton gradient via ATP synthase-proton driven [19]. It was shown that coupling respiration could extend the CLS in the reduced TORC1 signaling [19]. In addition, mitochondrial superoxide produced in TORC1 inhibition extended the CLS [18,19]. The reduced TOR signaling results in increased mitochondrial translation rates, coupled respiration, ROS detoxification, and life span by increasing the number OXPHOS subunit [18,19]. Previous data provided that OHPHOS components were upregulated such as Cox13p (subunit of Complex IV), Qcr7 (subunit of complex III), and Atp2p, Atp5p, and Atp7p (subunit of complex V/ATP synthase) [18]. Therefore, The CLS is extended in *tor1Δ* mutation in yeast through mitochondrial respiration by increasing the translation of mtDNA encodes the OXPHOS subunit system and through fewer ROS [19].

2. Materials and Methods

2.1 Yeast strains, media and growth conditions

The wild-type (WT) strain of *Saccharomyces cerevisiae* BY4742 (*MATα his3Δ1 leu2Δ0 lys2Δ0 ura3Δ0*) and the *tor1Δ* single-gene-deletion mutant strain in the BY4742 genetic background were obtained from Thermo Fisher scientific and Dharmacon. The cells were cultured in the nutrient rich liquid YEPD medium (1% yeast extract, 2% peptone) initially containing 2% (w/v) of glucose as carbon source. Cells culturing was performed at 30ºC with rotational shaking at 200 rpm in Erlenmeyer flasks. Each Erlenmeyer flask had a "flask volume/medium volume" ratio was 5:1.

Table 1. The strains of *S. Cerevisiae* used in this study.

Strain	Genotype	.Commercial source
WT	*MATα his3-Δ1 leu2-Δ0 lys2-Δ0 ura3-Δ0*	Thermo Fisher Scientific/Dharmacon
tor1Δ	*MATα his3-Δ1 leu2-Δ0 lys2-Δ0 ura3-Δ0 tor1Δ*	Thermo Fisher Scientific/Dharmacon

2.2 Clonogenic assay for measuring yeast chronological lifespan

A sample of cells was taken from a culture the following day the cell inoculation into liquid YEPD medium initially containing 2% (w/v) glucose. A fraction of the sample was diluted to determine the total number of cells using a hemocytometer. Another fraction of the cell sample was diluted, and serial dilutions of cells were plated in duplicate onto YEP plates containing 2% (w/v) glucose as carbon source. After 2 days of incubation at 30ºC, the number of colony-forming units (CFU) per plate was counted. The number of CFU was defined as the number of viable cells in a sample. For each culture, the percentage of viable cells was calculated as follows: (number of viable cells per ml/total number of cells per ml) × 100. The percentage of viable cells in the mid-logarithmic growth phase was set at 100%. The mean chronological lifespan of budding yeast culture is defined as the number of days needed to reach 50% cell viability. The maximum chronological lifespan is the number of days the culture needs to reach 10% cell viability.

2.3 Purification of mitochondria

Yeast cells cultured in liquid YEPD medium initially containing 2% (w/v) glucose were harvested at 3,000 × g for 5 min at room temperature. The cells were washed with water and resuspended in DTT buffer (100 mM Tris-H_2SO_4, pH 9.4, 10 mM dithiothreitol [DTT]). The cells were incubated in DTT buffer for 20 min at 30°C to weaken the cell wall. The cells were washed with Zymolyase buffer (1.2 M sorbitol, 20 mM potassium phosphate, pH 7.4) and pelleted by the centrifugation at 3,000 × g for 5 min at room temperature. The cells were incubated with 3 mg/g (wet weight) of Zymolyase-100T in 7 ml/g (wet weight) Zymolyase buffer for 45 min at 30°C in the rotational shaker at 75 rpm. The sample was then centrifuged at 2,200 × g at 4°C for 8 minutes that results in spheroplasts. These spheroplasts were washed in an ice-cold homogenization buffer (5 ml/g) (0.6 M sorbitol, 10 mM Tris-HCl, pH7.4, 1 mM EDTA, 0.2% (w/v) BSA) and centrifuged at 2,200 × g for 8 min at 4°C. The pelleted spheroplasts were homogenized in an ice-cold homogenization buffer using 15 strokes. Cell debris was removed by centrifuging the homogenates at 1,500 for 10 min at 4°C and then supernatant was centrifuged at 3,000 × g for 10 min at 4°C. The supernatant was centrifuged at 12,000 × g for 15 min at 4°C that contain mostly mitochondria in the pellet but also endoplasmic reticulum and vacuoles. The pellet was resuspended with 25 ml of ice-cold homogenization buffer. The remnant cell debris was pelleted by centrifuging the mitochondrial fraction at 3,000 × g for 5 min at 4°C. The supernatant was collected and centrifuged at 12,000 × g for 15 min at 4°C to obtain the crude mitochondrial pellet. This pellet was resuspended in 2 ml of SEM Buffer (250 mM sucrose, 1 mM EDTA, 10 mM MOPS, pH 7.2) and used to purify mitochondria further. A sucrose gradient was prepared by overlaying 1.5 ml of 60% sucrose with 4 ml of 32% sucrose, 1.5 ml of 23% sucrose and 1.5 ml of 15% sucrose (sucrose dissolved in EM buffer; 1 mM EDTA, 10 mM MOPS, pH 7.2). A 2-ml aliquot of the crude mitochondrial fraction in SEM buffer was applied to the gradient and placed in ultra-centrifuge at 134,000 × g (33,000 rpm) for 1 hours at 4°C in a vacuum (Rotor SW40Ti, Beckman). The purified mitochondria present at the 60%/32% sucrose interface were carefully removed and stored at -80°C.

2.4 Mitochondrial proteins extraction for digestion

2.4.1. Recovery of purified mitochondria from sucrose density gradient.

Purified mitochondria identified in the peak between 60% & 32% were further purified from the sucrose. This was done by adding 1 ml of purified mitochondria with 4 ml of ice-cold SEM buffer (250 mM sucrose, 1 mM EDTA, 10 mM Mops, pH 7.2). The sample was centrifuged at 9000 rpm for 45 minutes at 4°C to pellet the mitochondrial, and the supernatant was discarded. The pelleted mitochondria were resuspended in nanopore water and stored at -80°C.

2.4.2 Bradford protein assay

Bradford protein assay was used to measure the amount of protein in the samples. The BioMate160 spectrophotometer by Thermo Scientific was used to create the standard curve using different concentration solution of a bovine serum albumin (BSA). Each sample was prepared to measure its absorbance by adding 5 µl of the sample volume to 0.995 ml of 1X Bradford Reagent, vortexed in an Eppendorf tube and incubated for 10 minutes at room temperature. The absorbance of each sample was measured at 595 nm. Based on the measurement of protein concentrations in different samples, the volume of each sample needed was calculated to be taken for the precipitation of an equal amount of proteins.

2.4.3 Protein precipitation

A total of 15 µg of mitochondrial protein was taken from each sample used for the mass spectrometry-based proteomic analysis. The mitochondrial proteins were precipitated by adding trichloroacetic acid (TCA) with final concentration of 10% TCA and incubating the sample on ice for 30 minutes. The samples were centrifuged at 16,000x g for 12 minutes at 4°C to pellet the proteins and the supernatant was discarded. The pellet was incubated twice with 1.4 ml of 80% ice-cold acetone for 15 min to precipitate the proteins further and increase the pH of the sample. The samples were centrifuged at 16,000x g for 12 minutes at 4°C. The protein pellets were then dried in speed vacuum to evaporate the acetone for 5 minutes. The dry pellets were resuspended in the sample buffer for SDS-PAGE.

2.4.4. SDS-PAGE

The dry protein pellets in each sample were resuspended in SDS-PAGE sample buffer (2% SDS, 10% Glycerol, 5 % β-mercaptoethanol, 0.005% bromophenol blue in 62.5 mM Tris/HCl (pH 6.8)) to obtain a final protein concentration of 1μg/μl and incubated at room temperature overnight allowing the proteins to denature. Samples were loaded to a stacking gel (4% acrylamide/bis-acrylamide, 1% SDS and 0.125 M Tris/HCL, pH 6.8) for SDS-PAGE and running gel (12.5% acrylamide/bis-acrylamide, 1% SDS and 0.375 M Tris/HCL, pH 8.8). The protein bands run at 200V until the bands enter the running gel. The running gel was fixed with 40% ethanol and 10% acetic acid for 15 minutes, rinsed with water and stained with QC Colloidal Coomassie Blue for 1 hour. The gels were destained with water 4 times for 15 minutes intervals, each time on rotational shaker at 55 rpm. The destained gels were stored at 4°C until used for protein digestion and peptide extraction.

2.4.5. Protein digestion and peptide extraction

[Protocol provided by Concordia University's Centre for Biological Applications of Mass Spectrometry (CBAMS)]

Protein bands formed in the SDS-PAGE gel were cut out with a razor blade and are cut into small pieces (1×1×0.5 mm) placed into 1.5mL Eppendorf tubes. The gel pieces containing the mitochondrial proteome were reduced using 50 mM ammonium bicarbonate (NH_4HCO_3) in 10 mM dithiothreitol (DDT), vortexed, and incubated for 30 min at room temperature in the dark. The solution was discarded, and the gel pieces were vortexed and incubated in 50 mM iodoacetamide (IAA) for 30 min at room temperature in the dark. The solution was discarded, and the gel pieces were incubated in 50 mM NH_4HCO_3 at room temperature for 15 minutes. The solution was discarded, and the gel pieces were incubated in 25 mM NH_4HCO_3 with 5% acetonitrile (ACN) for 15 min at room temperature. The solution was discarded, and the gel pieces were incubated with 25 mM NH_4HCO_3 with 50% ACN for 30 minutes at room temperature. This step was repeated twice to confirm that all the staining has vanished. The solution was discarded, and the gel pieces were incubated for 10 minutes with 100% ACN. The gel pieces were dried at 37°C for 10 minutes and rehydrated with 0.01 μg/μl trypsin in 25 mM ABC solution and incubated overnight at 30°C. The gel pieces were incubated in 60% ACN and 0.5% formic acid for 15 minutes, and the supernatant was collected. This step was repeated twice, and the gel pieces were discarded. The

supernatant was saved, further dried in SpeedVac for several hours forming peptide pellet in the Eppendorf tubes, and stored at -20°C until preparation for Mass Spectrometry (MS) Analysis.

2.5 Mass spectrometric identification of mitochondrial proteins

Dried peptides in each sample were reconstituted in 2% ACN and 1% formic acid to inject 200ng. The proteins are identified by reverse-phase high-performance liquid chromatography coupled to mass spectrometry (RP-HPLC-MS/MS) using EASY-nLC^{TM} coupled to LTQ Orbitrap. 3-µl aliquots of peptides were separated in the ACN gradient using a 100-µM capillary column packed with C18 mobile phase.

Once the mass spectrometric separation of peptides using the LTQ Orbitrap was completed, the raw mass spectrometry data file obtained by Xcalibur was analyzed using the Thermo Proteome Discoverer application (version PD2.4). The Proteome Discoverer was used to identify individual proteins by comparing the raw data of mass spectra of digested fragments to peptides' mass spectra within the Uniprot FASTA database to search for Saccharomyces cerevisiae databases, using custom workflows by CBAMS. The analysis by the Proteome Discoverer coupled to the FASTA database was enabled by using the peak-finding search engine SEQUEST. The SEQUEST engine processes MS data using a peak-finding algorithm to search the raw data for generating a peak probability list with relative protein abundances. The proteome discoverer software was used to calculate the grouped abundance (relative abundance) of mitochondrial proteins in 2 biological replicates (2 independent experiment) by taking the arithmetic mean of all the replicate abundance values within a sample group.

The following settings of the SEQUEST search wizard within the Proteome Discoverer application were used:

Database: Uniprot_sprot FASTA

Enzyme: Trypsin

Missed Cleavages: The maximum number of internal cleavage sites per peptide fragment acceptable for an enzyme to miss during proteolytic digest. The default value of 2 was used.

2.6. Comparing the abundance of proteins in mitochondria purified from WT and *tor1Δ* cells

The "Proteome Discoverer" software was used to calculate the abundance of each protein as the sum of the peak intensities of all its unique tryptic peptides identified from the raw mass spectrometry data [1]. This method is a common standard approach for proteomics by comparing protein concentrations in various biological samples with the help of mass spectrometry-assisted proteomics [1]. The values for all mitochondrial proteins identified in the WT and *tor1Δ* strains were plotted on the logarithmic scales. Proteins that are downregulated [i.e., for which the ratios of protein abundance of tor1Δ /protein abundance of WT (from peptides' peak intensities) are lower than 0.5] or upregulated (i.e., for which these ratios exceed 2.0) in mitochondria of the *tor1Δ* mutant strain were plotted on the scatter plots. Proteins whose concentration are not changed (i.e., the above ratios are between 0.5 and 2.0) in mitochondria of the *tor1Δ* mutant strain were shown on the scatter plots. The "Proteome Discoverer" PD2.4 calculated the arithmetic means of two independent experiments referred to as grouped abundance and the aging-associated changes in the relative abundance of different proteins within mitochondria of the *tor1Δ* mutant strain versus those within mitochondria of the WT strain.

3. Results and discussion

3.1 The *tor1Δ* mutation extends the CLS of budding yeast

The longevity of chronological aging S. cerevisiae was extended by single-gene deletion mutation *tor1Δ* (Figure 1). As Figure 1 shows, the *tor1Δ* extends both the mean and maximum CLS of budding yeast. As discussed in the introduction section of my thesis, it was hypothesized that the *tor1Δ* mutation affects several mitochondrial processes that contribute to the functional state of mitochondria. These mitochondrial processes include mitochondrial ROS production, mitochondrial respiration and mitochondrial dynamics. Therefore, I hypothesized that the *tor1Δ*-inflicted alterations in mitochondrial functionality could extend budding yeast's CLS.

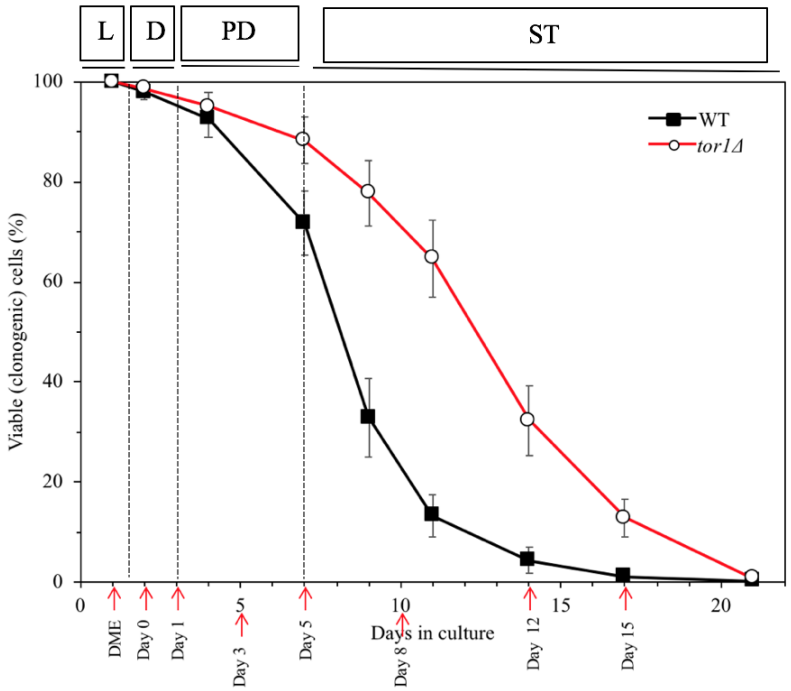

Figure 1. The *tor1Δ* mutation extends the longevity of chronological aging in budding yeast. WT and *tor1Δ* mutant were cultured in YEPD (1% yeast extract and 2% peptone) medium initially containing 2% glucose. The CLS was monitored as described in Materials and Methods. The viability curve analysis is based on the data of 3 independent experiments performed by Pamela Dakik and undergraduate students. Abbreviation: L, D, PD, ST, and DME, logarithmic, diauxic, post-diauxic, stationary growth phases and mid exponential day respectively.

3.2 The *tor1Δ* mutation alter the mitochondrial proteome in an age-related manner

I tested the hypothesis on *tor1Δ* mutation that alters the mitochondrial functionality and, thus, extends yeast CLS because it could change the concentrations of mitochondrial proteins. Mitochondria were purified and precipitated mitochondrial proteins from differently aged WT and *tor1Δ* mutant cells cultured in YEPD medium with 2% glucose. To get a broader view of the mitochondrial proteome changes, each sample was further analyzed using mass spectrometry-based quantitative proteomics to identify mitochondrial proteins that are up- or down-regulated by the *tor1Δ* mutation and to assess the relative abundance of these proteins.

I found that the *tor1Δ* mutation alters the relative concentrations of many mitochondrial proteins in yeast cells (Table 2; Figures 2.1A-2.1H). Notably, the numbers of mitochondrial proteins down-regulated (Figure 2.2 A-H) or up-regulated (Figure 2.3 A-H) by the *tor1Δ* mutation increased with the age of budding yeast cells (*i.e.*, in an age-related manner).

Table 2. The numbers of mitochondrial proteins that were upregulated or downregulated in *tor1Δ* mutant cells on different days of cell culturing. A total of 675-715 mitochondrial proteins were identified and quantitatively assessed per sample. A total number of mitochondrial proteins that were (*i.e.*, more than 2 folds) up- or (*i.e.*, less than 0.5 folds) down-regulated by the *tor1Δ* mutation are displayed on the red or blue background color respectively.

Timepoint (Days)	Protein concentration	Total Number of mitochondrial proteins that are up- or down-regulated by the *tor1Δ* mutation	Total Number of Proteins per sample
DME	Upregulated	20	703
	Downregulated	3	
Day 0	Upregulated	14	685
	Downregulated	7	
Day 1	Upregulated	41	705
	Downregulated	14	
Day 3	Upregulated	66	691
	Downregulated	21	
Day 5	Upregulated	70	697
	Downregulated	12	
Day 8	Upregulated	58	715
	Downregulated	13	
Day 12	Upregulated	54	675
	Downregulated	14	
Day 15	Upregulated	94	679
	Downregulated	24	

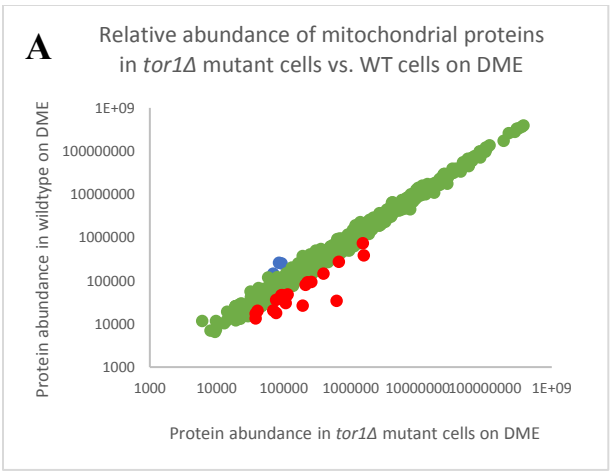
A
Relative abundance of mitochondrial proteins in tor1Δ mutant cells vs. WT cells on DME
Protein abundance in wildtype on DME
Protein abundance in tor1Δ mutant cells on DME
1E+09
100000000
10000000
1000000
100000
10000
1000
1000
10000
100000
1000000
10000000
100000000
1E+09

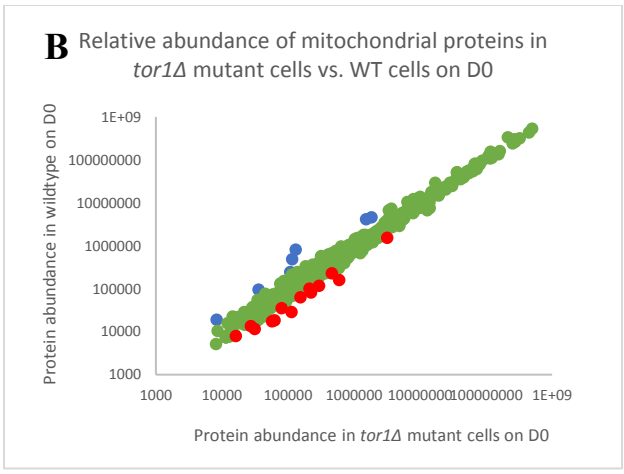
B
Relative abundance of mitochondrial proteins in tor1Δ mutant cells vs. WT cells on D0
Protein abundance in wildtype on D0
Protein abundance in tor1Δ mutant cells on D0
1E+09
100000000
10000000
1000000
100000
10000
1000
1000
10000
100000
1000000
10000000
100000000
1E+09

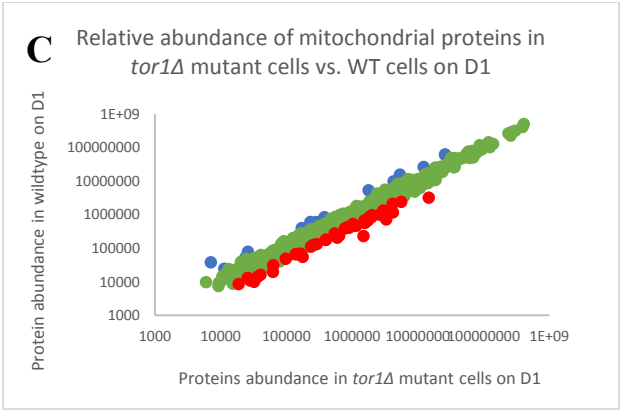
C
Relative abundance of mitochondrial proteins in tor1Δ mutant cells vs. WT cells on D1
Protein abundance in wildtype on D1
Proteins abundance in tor1Δ mutant cells on D1
1E+09
100000000
10000000
1000000
100000
10000
1000
1000
10000
100000
1000000
10000000
100000000
1E+09

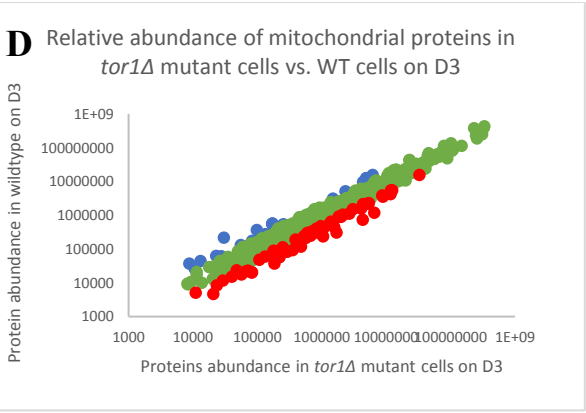
D
Relative abundance of mitochondrial proteins in tor1Δ mutant cells vs. WT cells on D3
Protein abundance in wildtype on D3
Proteins abundance in tor1Δ mutant cells on D3
1E+09
100000000
10000000
1000000
100000
10000
1000
1000
10000
100000
1000000
10000000
100000000
1E+09

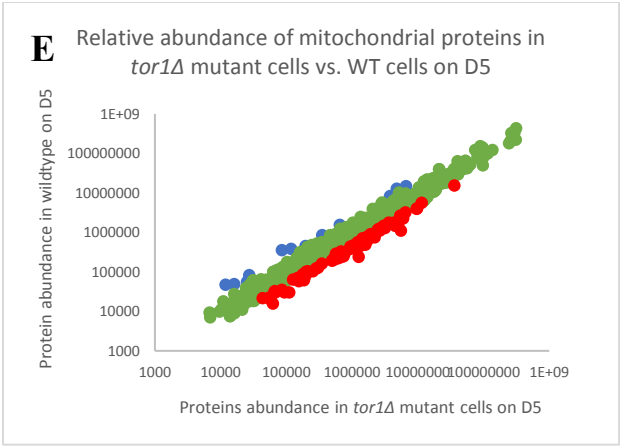
E
Relative abundance of mitochondrial proteins in tor1Δ mutant cells vs. WT cells on D5
Protein abundance in wildtype on D5
Proteins abundance in tor1Δ mutant cells on D5
1E+09
100000000
10000000
1000000
100000
10000
1000
1000
10000
100000
1000000
10000000
100000000
1E+09

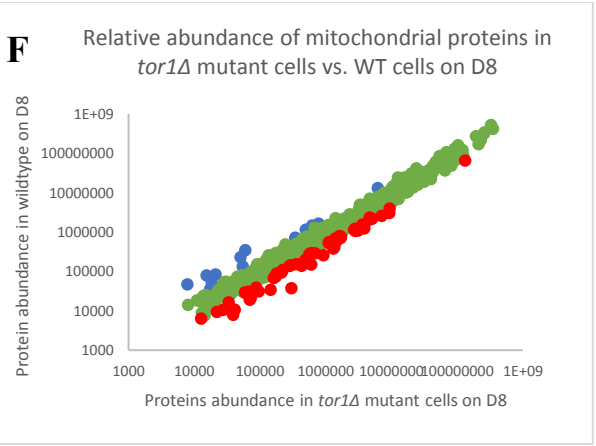
F
Relative abundance of mitochondrial proteins in tor1Δ mutant cells vs. WT cells on D8
Protein abundance in wildtype on D8
Proteins abundance in tor1Δ mutant cells on D8
1E+09
100000000
10000000
1000000
100000
10000
1000
1000
10000
100000
1000000
10000000
100000000
1E+09

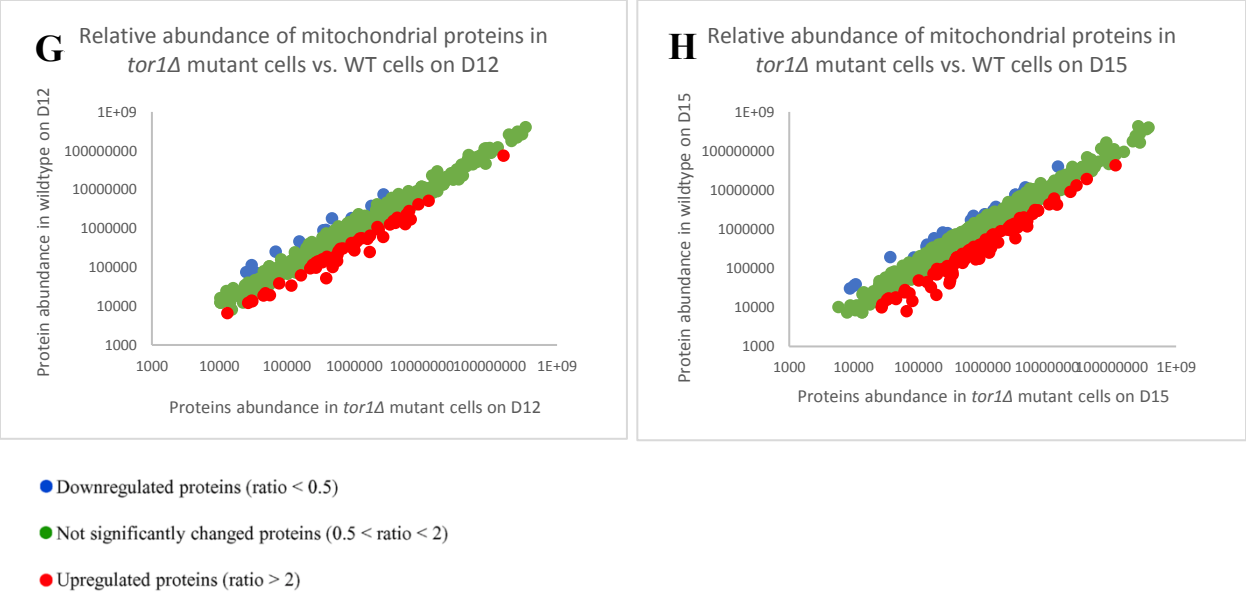

Figure 2.1. The *tor1Δ* mutation alters the relative concentrations of many mitochondrial proteins in an age-related manner. Wildtype and *tor1Δ* mutant cells were cultured in YEPD (1% yeast extract and 2% peptone) medium initially containing 2% glucose. Cells were recovered on days DME, day 0, 1, 3, 5, 8, 12 and 15 of cell culturing were used to purify mitochondria as described in Materials and Methods. Mass spectrometry-based identification and quantitation of mitochondrial proteins recovered from these cells, and the calculation of the relative abundance of mitochondrial proteins in a pair of analyzed datasets (*i.e.* in the datasets of age-matched WT cells cultured with *tor1Δ* mutant cells cultured), were performed using PD2.4 as described in Materials and Methods. (**A-H**) Scatter plots comparing the relative abundance of mitochondrial proteins between specified datasets were plotted on a log-log scale. Data are presented on the number of mitochondrial proteins as means of 2 independent experiments.

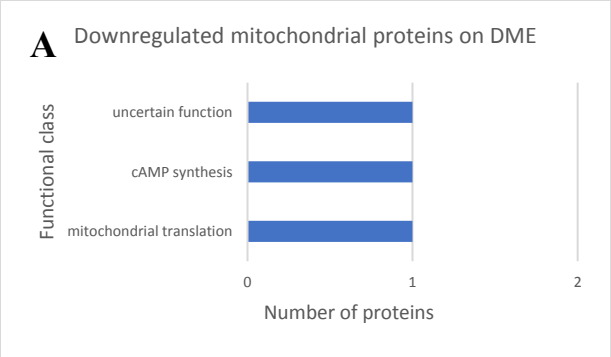
A
Downregulated mitochondrial proteins on DME
Functional class
uncertain function
cAMP synthesis
mitochondrial translation
0
1
2
Number of proteins

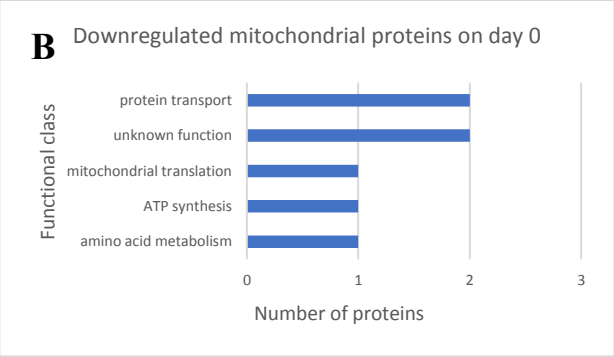
B
Downregulated mitochondrial proteins on day 0
Functional class
protein transport
unknown function
mitochondrial translation
ATP synthesis
amino acid metabolism
0
1
2
3
Number of proteins

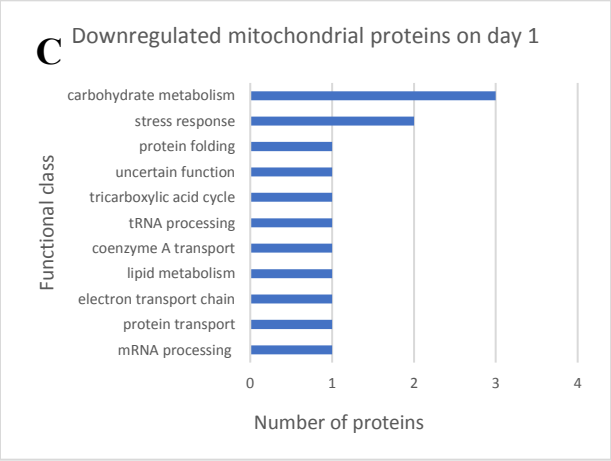
C
Downregulated mitochondrial proteins on day 1
Functional class
carbohydrate metabolism
stress response
protein folding
uncertain function
tricarboxylic acid cycle
tRNA processing
coenzyme A transport
lipid metabolism
electron transport chain
protein transport
mRNA processing
0
1
2
3
4
Number of proteins

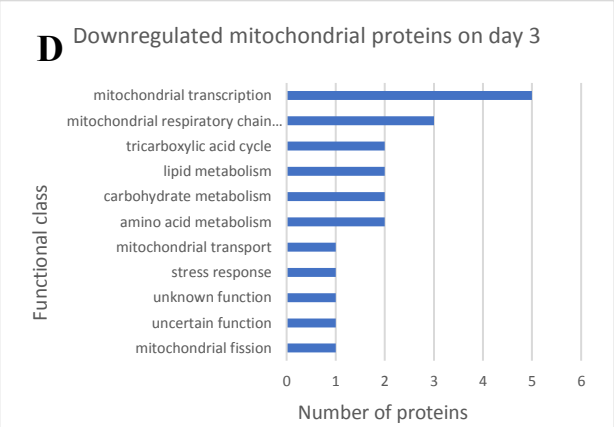
D
Downregulated mitochondrial proteins on day 3
Functional class
mitochondrial transcription
mitochondrial respiratory chain...
tricarboxylic acid cycle
lipid metabolism
carbohydrate metabolism
amino acid metabolism
mitochondrial transport
stress response
unknown function
uncertain function
mitochondrial fission
0
1
2
3
4
5
6
Number of proteins

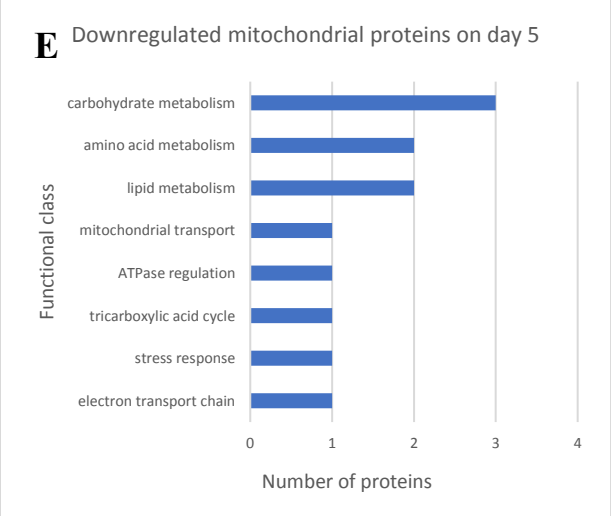
E
Downregulated mitochondrial proteins on day 5
Functional class
carbohydrate metabolism
amino acid metabolism
lipid metabolism
mitochondrial transport
ATPase regulation
tricarboxylic acid cycle
stress response
electron transport chain
0
1
2
3
4
Number of proteins

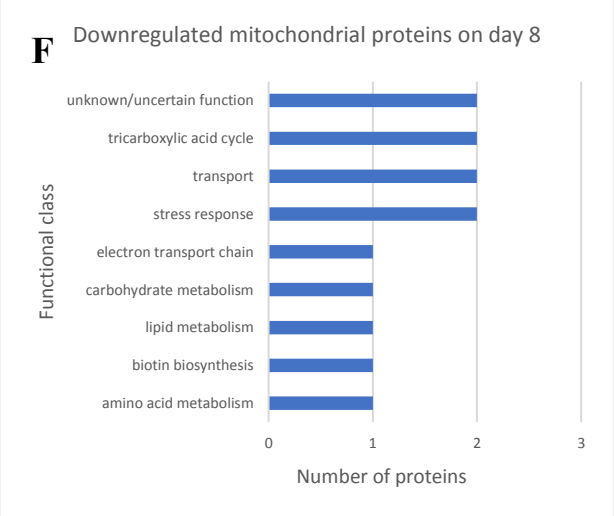
F
Downregulated mitochondrial proteins on day 8
Functional class
unknown/uncertain function
tricarboxylic acid cycle
transport
stress response
electron transport chain
carbohydrate metabolism
lipid metabolism
biotin biosynthesis
amino acid metabolism
0
1
2
3
Number of proteins

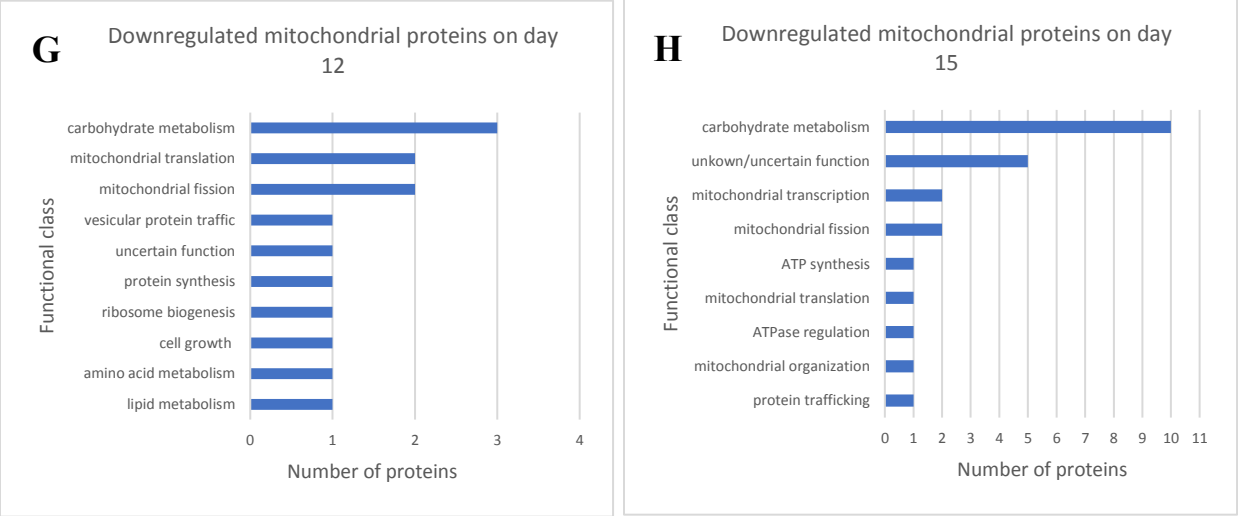

Figure 2.2. The *tor1Δ* mutation decreases the relative concentrations of many mitochondrial proteins in an age-related manner. Wildtype and *tor1Δ* mutant cells were cultured in YEPD (1% yeast extract and 2% peptone) medium initially containing 2% glucose. Cells were recovered on DME, day 0, 1, 3, 5, 8, 12 and 15 of cell culturing were used to purify mitochondria as described in Materials and Methods. Mass spectrometry-based identification and quantitation of proteins recovered from these cells, and the calculation of the relative abundance of mitochondrial proteins in a pair of analyzed datasets (*i.e.* in the datasets of age-matched WT cells cultured and *tor1Δ* mutant cells cultured), were performed using PD2.4 as described in Materials and Methods. (**A**-**H**) Bar plots showing the functional classes of mitochondrial proteins that were downregulated (*i.e.*, whose abundance ratio was lower than 0.5 folds) on different days of cell culturing. Data are presented on the number of mitochondrial proteins as means of 2 independent experiments.

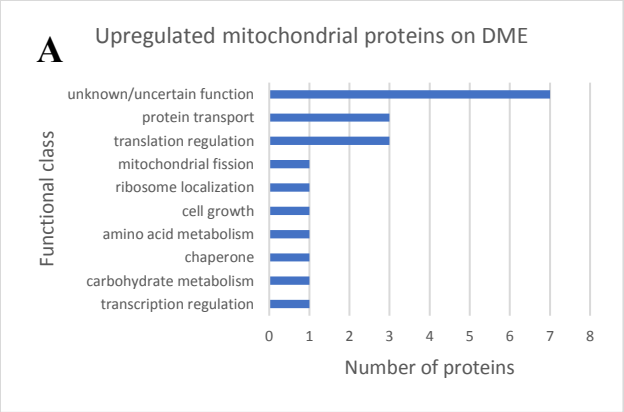
A
Upregulated mitochondrial proteins on DME
unknown/uncertain function
protein transport
translation regulation
mitochondrial fission
ribosome localization
cell growth
amino acid metabolism
chaperone
carbohydrate metabolism
transcription regulation
Functional class
0 1 2 3 4 5 6 7 8
Number of proteins

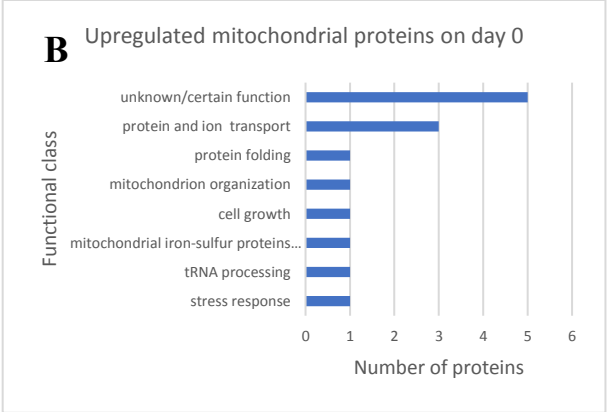
B
Upregulated mitochondrial proteins on day 0
unknown/certain function
protein and ion transport
protein folding
mitochondrion organization
cell growth
mitochondrial iron-sulfur proteins...
tRNA processing
stress response
Functional class
0 1 2 3 4 5 6
Number of proteins

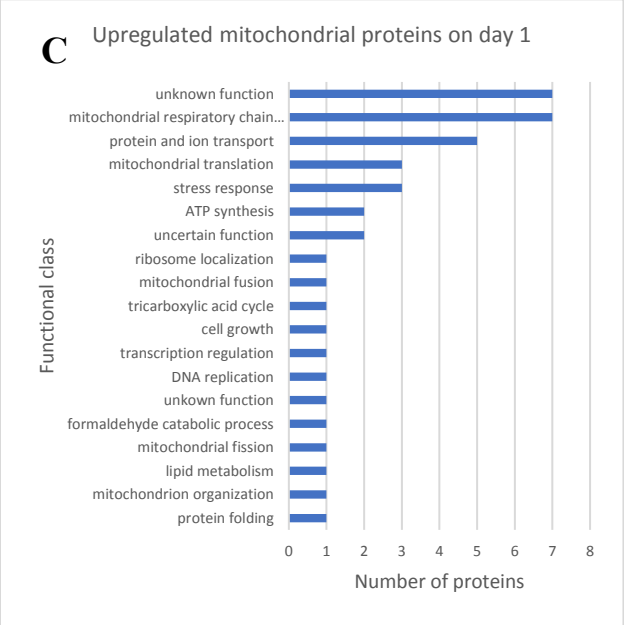
C
Upregulated mitochondrial proteins on day 1
unknown function
mitochondrial respiratory chain...
protein and ion transport
mitochondrial translation
stress response
ATP synthesis
uncertain function
ribosome localization
mitochondrial fusion
tricarboxylic acid cycle
cell growth
transcription regulation
DNA replication
unkown function
formaldehyde catabolic process
mitochondrial fission
lipid metabolism
mitochondrion organization
protein folding
Functional class
0 1 2 3 4 5 6 7 8
Number of proteins

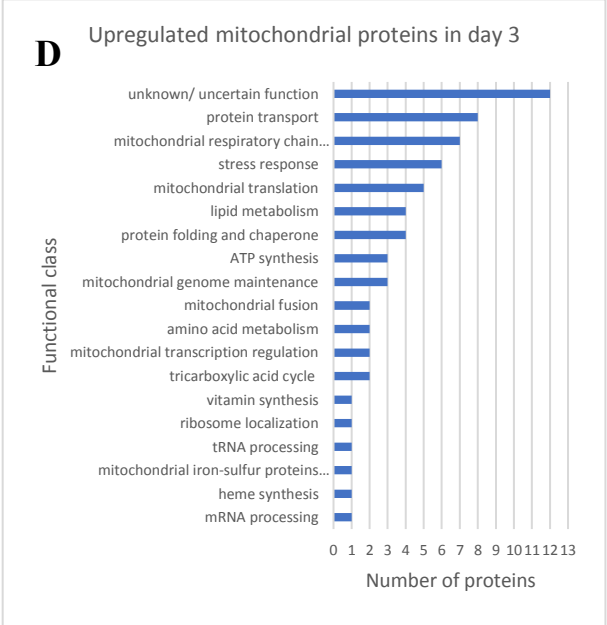
D
Upregulated mitochondrial proteins in day 3
unknown/ uncertain function
protein transport
mitochondrial respiratory chain...
stress response
mitochondrial translation
lipid metabolism
protein folding and chaperone
ATP synthesis
mitochondrial genome maintenance
mitochondrial fusion
amino acid metabolism
mitochondrial transcription regulation
tricarboxylic acid cycle
vitamin synthesis
ribosome localization
tRNA processing
mitochondrial iron-sulfur proteins...
heme synthesis
mRNA processing
Functional class
0 1 2 3 4 5 6 7 8 9 10 11 12 13
Number of proteins

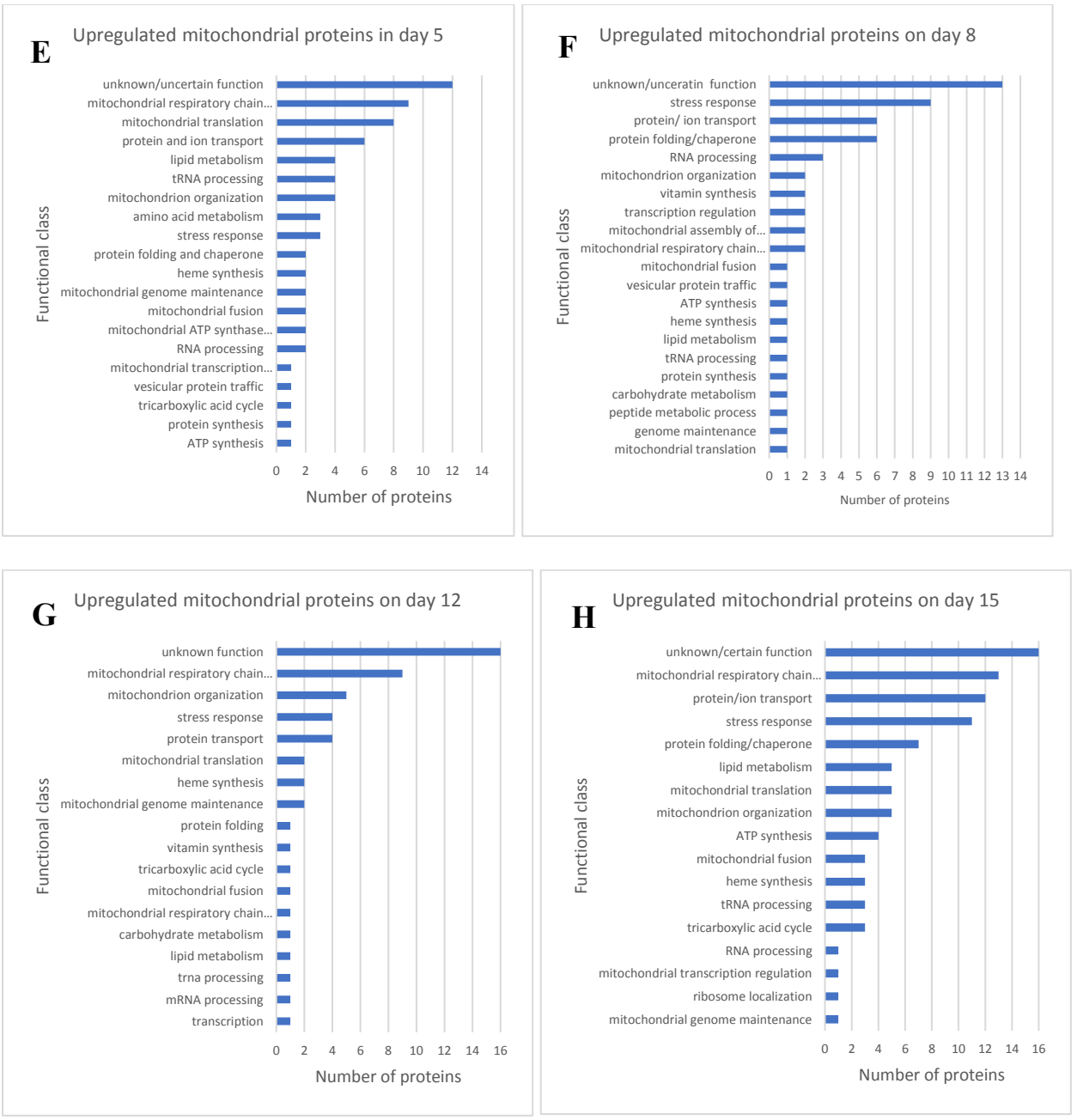

Figure 2.3. The *tor1Δ* mutant increases the relative concentrations of many mitochondrial proteins in an age-related manner. Wildtype and *tor1Δ* mutant cells were cultured in YEPD (1% yeast extract and 2% peptone) medium initially containing 2% glucose. Cells were recovered on DME, day 0, 1, 3, 5, 8, 12 and 15 of cell culturing were used to purify mitochondria as described in Materials and Methods. Mass spectrometry-based identification and quantitation of proteins recovered from these cells, and the calculation of the relative abundance of mitochondrial proteins in a pair of analyzed datasets (*i.e.* in the datasets of age-matched WT cells cultured and *tor1Δ* mutant cells cultured), were performed using PD2.4 as described in Materials and Methods. (**A**-**H**) Bar plots showing the functional class of mitochondrial proteins that were up-regulated (*i.e.*, whose abundance ratio was more than 2 folds) on different days of cell culturing. Data are presented on the number of mitochondrial proteins as means of 2 independent experiments.

3.3 Principal component analysis plot on mitochondrial proteins

The principal component analysis plot (PCA) was used to compare the mitochondrial proteome of wild-type cells to the mitochondrial proteome of aged-matched *tor1Δ* mutant in cells. These cells were recovered on different days of culturing and purified mitochondrial proteins from two independent experiments. Each sample was subjected to the mass-spectrometry-based proteomics and then PCA plots were generated from Proteome Discoverer (version PD2.4) software. The data in the principal component analysis that are close to each other are most similar proteomes. The first PCA is 29.7% of the data's variability, and the second PCA is 15.6% of the data's variability that was plotted by the proteome discoverer software (PD2.4) from spectra. The PCA plot was performed according to the mitochondrial proteome of two different biological repeats of the experiment (Figure 3.1, Figure 3.4), different time points in days (Figure 3.2, Figure 3.4) and a pair of different strains (*i.e.*, WT and *tor1Δ*) (Figure 3.3, Figure 3.4).

The mitochondrial proteome from cells recovered on DME, day 0 and day 1 was clustered on PCA plots much closer to each other than those of chronologically older cells (Figure 3.2). The mitochondrial proteome points from the wild-type cells were separated compared to the mitochondrial proteome from *tor1Δ* mutant (Figure 3.3). According to the PCA plot, the mitochondrial proteome in the wild-type cells are clustered mostly on the right and the mitochondrial proteome in *tor1Δ* mutant cells are clustered on the left on most days of cell culturing except for DME (Figure 3.3). The pattern observed on the PCA plot are from 2 biological replicates (two independent experiments), each including cell culturing, mitochondria purification, mass spectrometry-based proteomics, and the PCA of mitochondrial proteins illustrates that the mitochondrial proteome in 2 independent experiments were reasonably close to each other (Figure 3.1, Figure 3.4). In sum, the findings of the PCA plot analysis provide conclusive evidence that the mitochondrial proteomes in the wildtype cells differ from the mitochondrial proteins in the *tor1Δ* mutant purified from yeast cells except for DME (Figure 3.4).

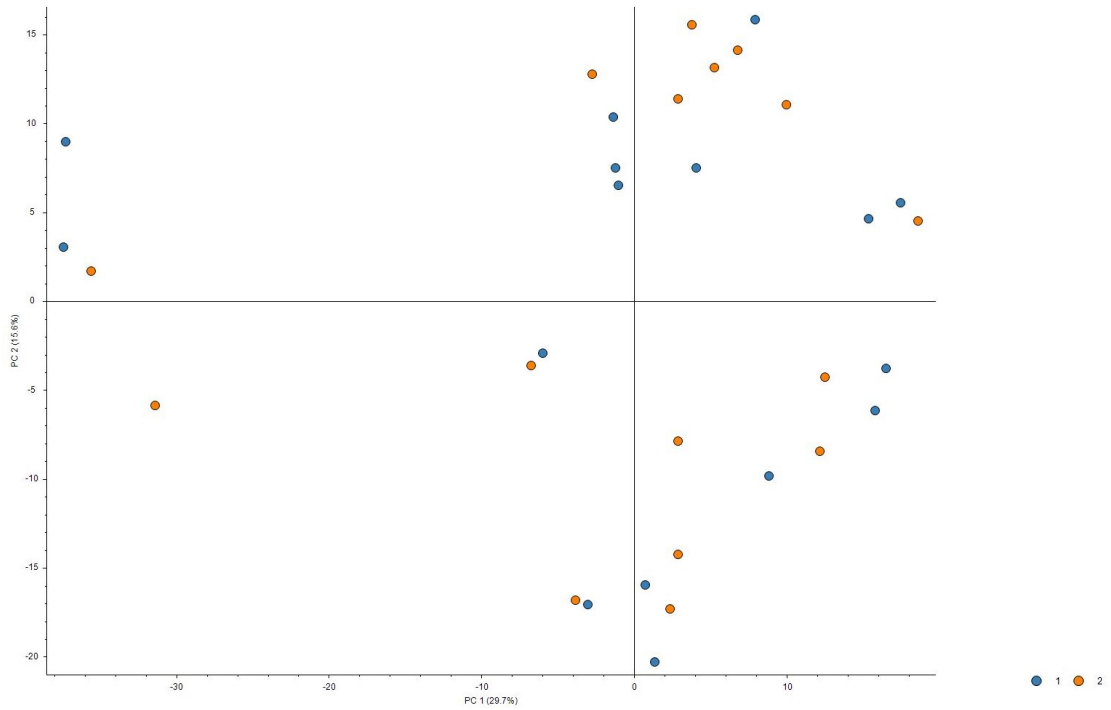

Figure 3.1. The PCA plot of mitochondrial proteomes found in two biological replicates (independent experiments) performed with wildtype and *tor1Δ* mutant cells. The data of different biological replicates (independent experiments) are displayed in different colors.

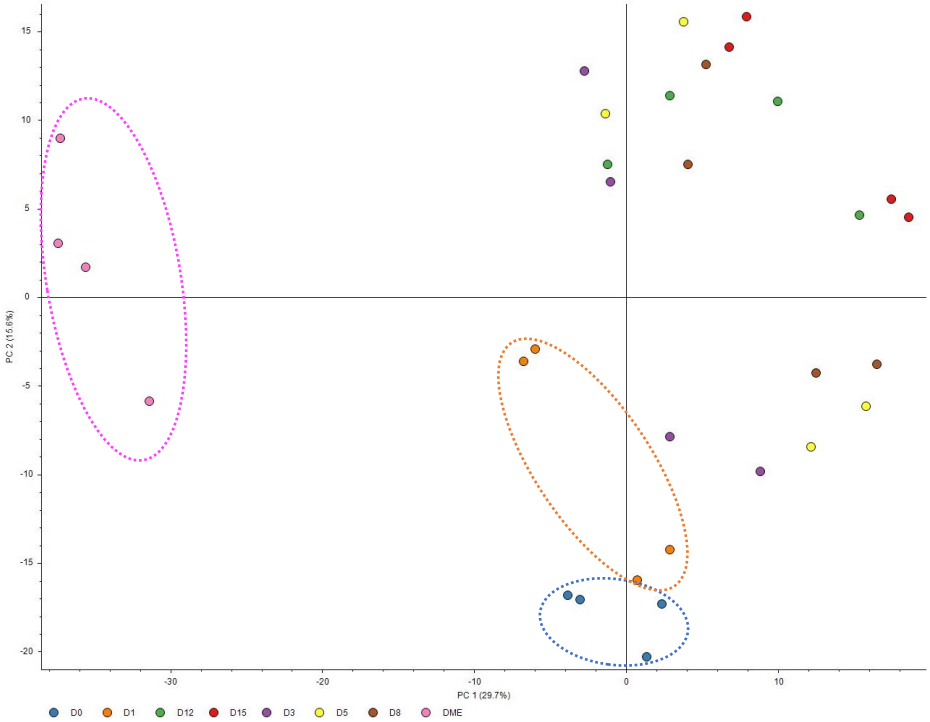

Figure 3.2. The PCA plot of mitochondrial proteomes recovered from different days of culturing (age) performed with wildtype and *tor1Δ* mutant cells in two biological replicates. The data on different cell culturing days are displayed in different colors and was obtained from thermo proteome discoverer PD2.4.

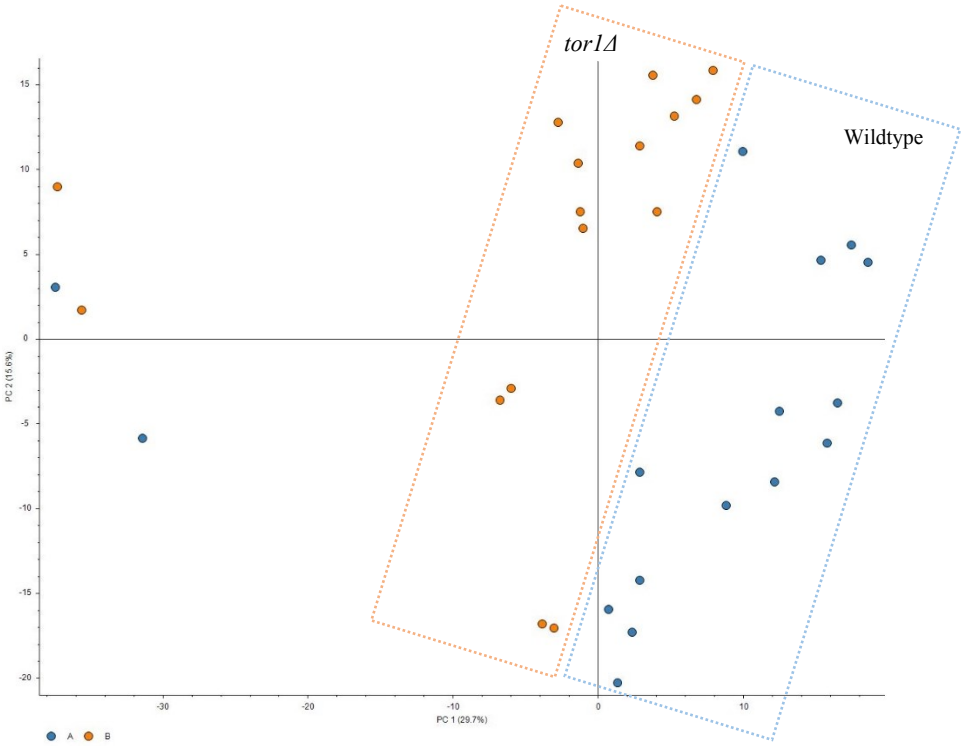

Figure 3.3. The PCA plot of mitochondrial proteomes found in different strain type performed with wildtype (A) and *tor1Δ* mutant (B) cells recovered on different days of culturing in two biological replicates. The data for two different strains is displayed in different colors.

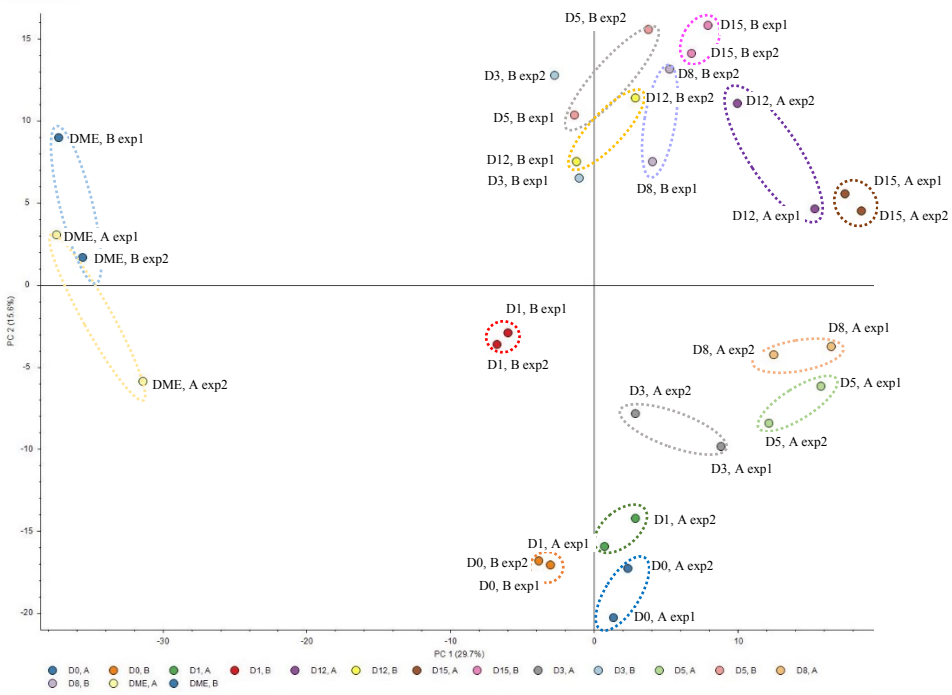

Figure 3.4. The PCA plot for the mitochondrial proteomes found in two biological replicates performed with Wildtype (A) and *tor1Δ* mutant (B) cells recovered on different days of culturing. The data for the two-biological replicate (independent experiment), two different strains, and different days of culture are displayed in different colors were obtained from thermo proteome discoverer PD2.4.

3.4 The *tor1Δ* mutation causes a global remodeling of the mitochondrial proteome by upregulating and downregulating in an age-related manner many mitochondrial proteins that perform various functions.

In support of my hypothesis, the *tor1Δ* mutation elicits changes in the relative concentrations of many mitochondrial proteins implicated in some key aspects of mitochondrial functionality.

Specifically, I found that the *tor1Δ* mutation increases the abundance of mitochondrial proteins involved in the following processes: 1) mitochondrial fusion (Figure 4.1A), 2) mitochondrial organization except for TMA19 (Figure 4.1B, 4.1D), 3) protein folding and refolding in mitochondria (Figure 4.2A), 4) protein and ion transport from and into mitochondria (Figure 4.2B), 5) lipid metabolism in mitochondria (Figure 4.2D), 6) ROS detoxification and protein protection from ROS-inflicted oxidative damage in mitochondria (Figure 4.2E), 7) the mitochondrial electron transport chain (ETC) and oxidative phosphorylation (OXPHOS) except for INH that is a negative regulator to ATPase (Figures 4.3A, Figures 4.3B), 8) heme synthesis in mitochondria and heme attachment to mitochondrial proteins (Figure 4.3C), 9) the mitochondrial tricarboxylic acid (TCA) cycle (Figure 4.3D), and 10) protein translation in mitochondria except for GRS1 (Figures 4.4A, Figure 4.4B).

Moreover, I found that the *tor1Δ* mutation decreases the abundance of mitochondrial proteins involved in mitochondrial fission (division) (Figure 4.1C) and carbohydrate metabolism in mitochondria at the stationary growth phase (Figure 4.2C).

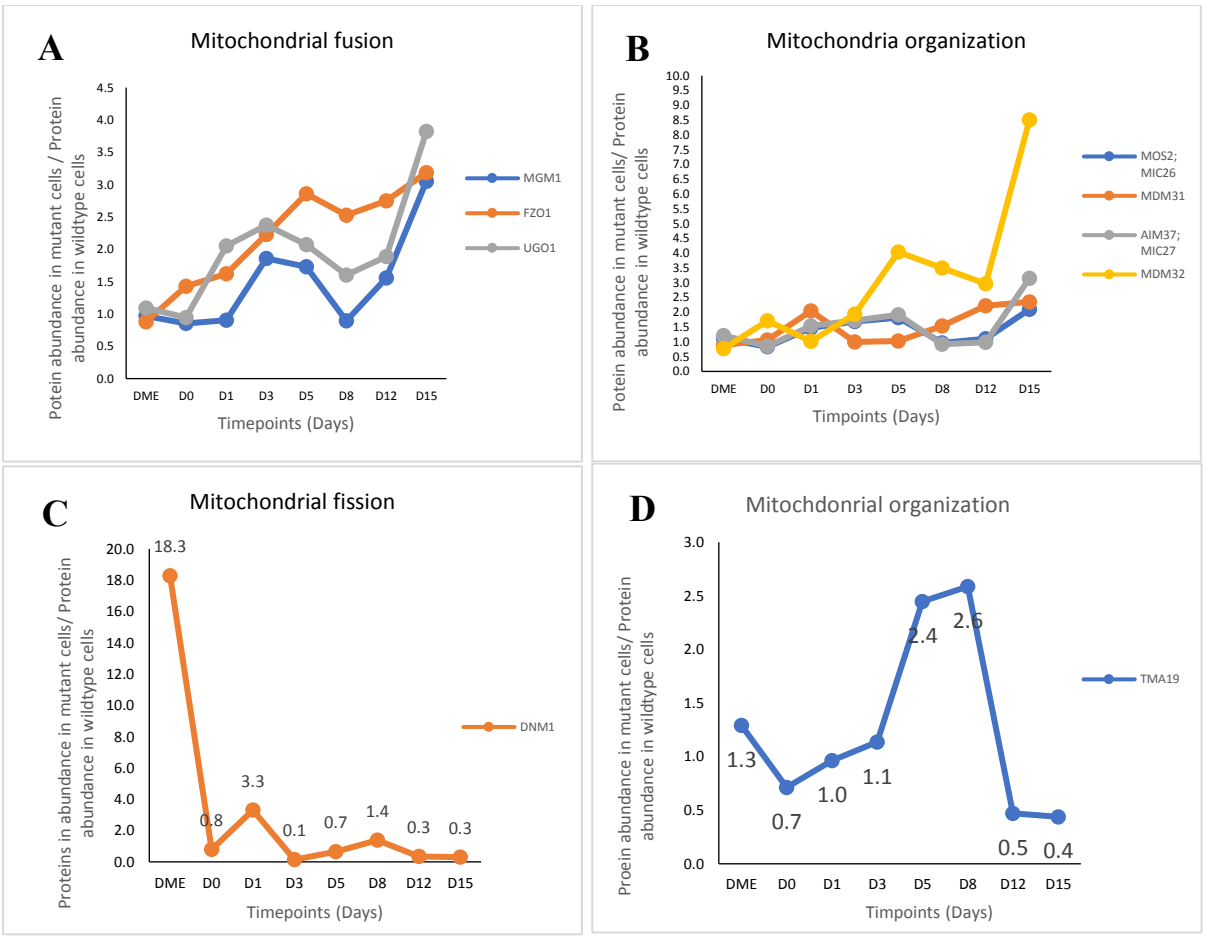

Figure 4.1. The *tor1Δ* mutation alters the abundance of proteins involved in mitochondrial fusion, fission and mitochondrial organization. WT and *tor1Δ* mutant cells were cultured in the YEPD (1% yeast extract and 2% peptone) medium initially containing 2% glucose. Cells were recovered on DME, day 0, 1, 3, 5, 8, 12 and 15 of cell culturing were used to purify mitochondria as described in Materials and Methods. Mass spectrometry-based identification and quantitation of mitochondrial proteins recovered from these cells, and the calculation of the relative abundance of mitochondrial proteins in a pair of analyzed datasets (i.e. in the datasets of age-matched WT cells cultured with *tor1Δ* mutant cells cultured), were performed using PD2.4 as described in Materials and Methods. The 2-fold increase in the ratio "protein abundance of tor1Δ /protein abundance of WT" represents the upregulation and lower than 0.5 folds in the ratio represent the downregulation of the protein. These proteins include the following ones: (**A**) mitochondrial proteins involved in mitochondrial fusion, (**B**) upregulated mitochondrial organization, (**C**) downregulation of mitochondrial fission, and (**D**) downregulated a protein responsible for mitochondrial organization. Data are presented as mean values of 2 independent experiments.

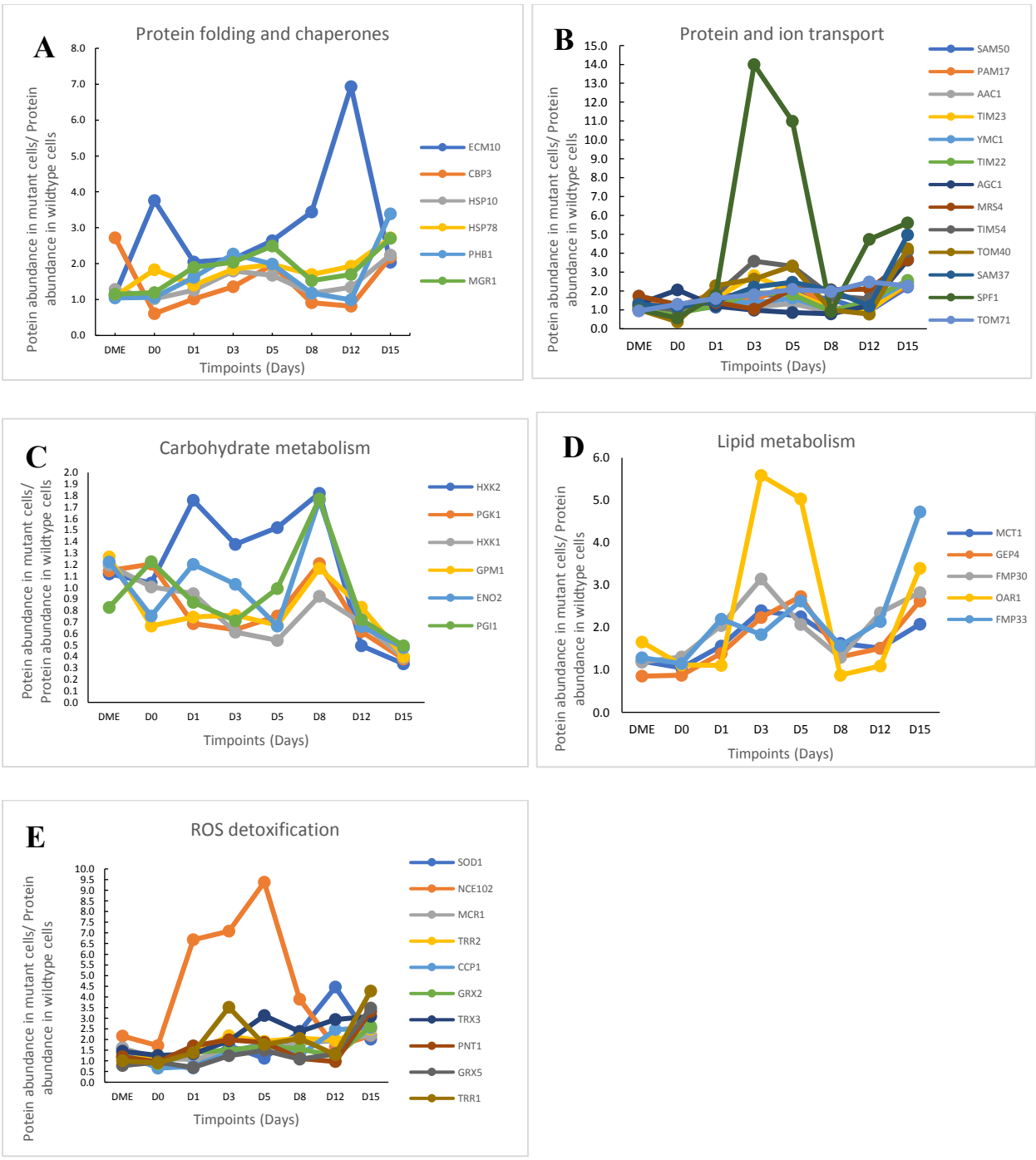

Figure 4.2. The *tor1Δ* mutation alters the abundance of mitochondrial proteins implicated in protein folding, protein and ion transport into mitochondria, carbohydrate metabolism, lipid metabolism and ROS detoxification. WT and *tor1Δ* mutant cells were cultured in the YEPD (1% yeast extract and 2% peptone) medium initially containing 2% glucose. Cells were recovered on DME, day 0, 1, 3, 5, 8, 12 and 15 of cell culturing were used to purify mitochondria as described in Materials and Methods. Mass spectrometry-based identification and quantitation of mitochondrial proteins recovered from these cells, and the calculation of the relative abundance of mitochondrial proteins in a pair of analyzed datasets (i.e. in the datasets of age-matched WT cells cultured with *tor1Δ* mutant cells cultured), were performed using PD2.4 as described in Materials and Methods. The 2-fold increase in the ratio "protein abundance of tor1Δ

/protein abundance of WT" represents the upregulation and lower than 0.5 folds in the ratio represent the downregulation of the protein. These proteins include the following ones: (**A**) mitochondrial proteins involved in chaperones involved in the folding and refolding of other mitochondrial proteins, (**B**) components of the mitochondrial protein transport machinery, (**C**) proteins involved in carbohydrate metabolism that were downregulated, (**D**) proteins catalyze the biosynthesis of some lipids for the mitochondrial membrane and fatty acids, (**E**) ROS detoxification and oxidative stress protection enzymes. Data are presented as mean values of 2 independent experiments.

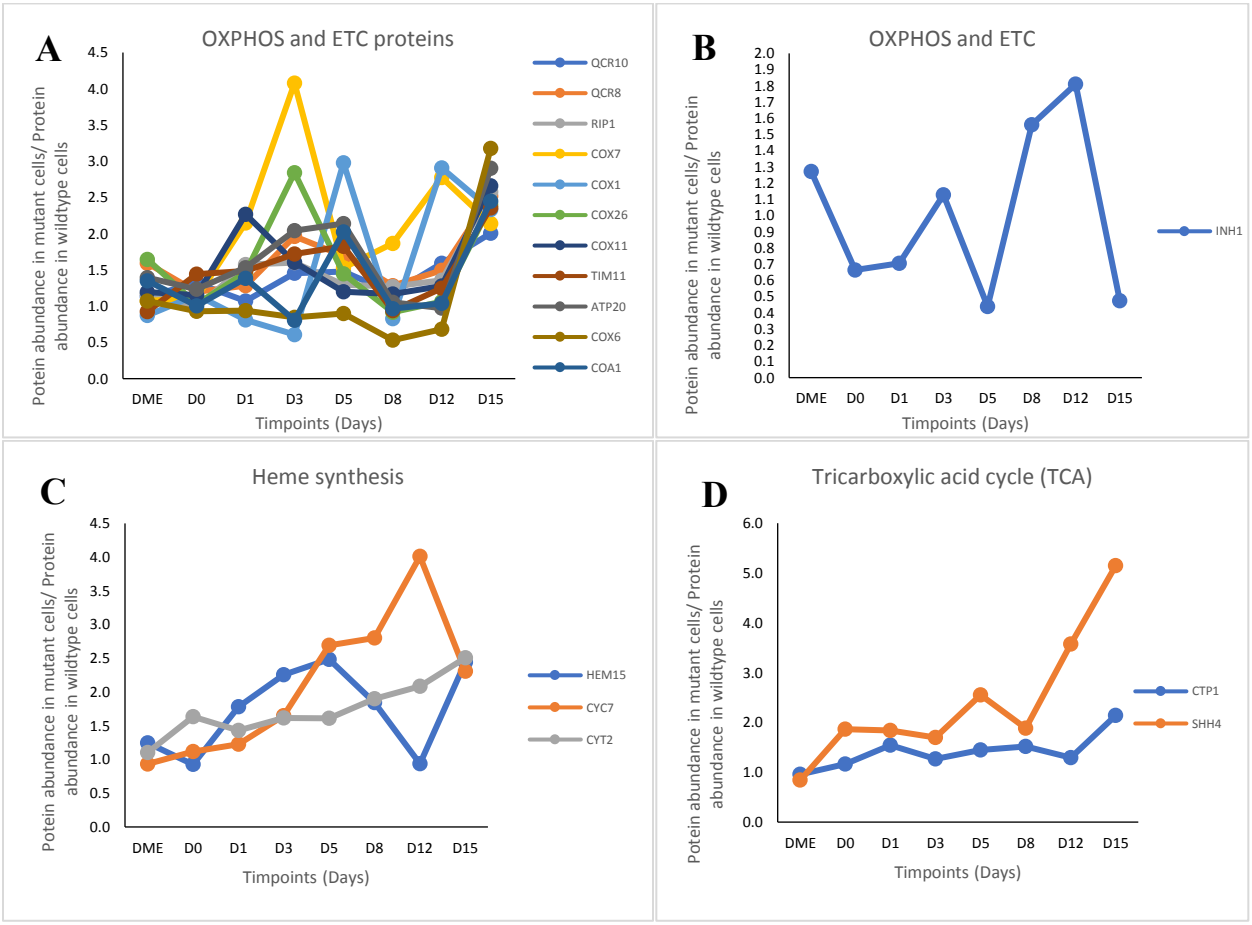

Figure 4.3. The tor1Δ mutation alters the abundance of mitochondrial proteins involved in the OXPHOS, ETC, heme synthesis and the tricarboxylic acid cycle. WT and *tor1Δ* mutant cells were cultured in the YEPD (1% yeast extract and 2% peptone) medium initially containing 2% glucose. Cells were recovered on DME, day 0, 1, 3, 5, 8, 12 and 15 of cell culturing were used to purify mitochondria as described in Materials and Methods. Mass spectrometry-based identification and quantitation of mitochondrial proteins recovered from these cells, and the calculation of the relative abundance of mitochondrial proteins in a pair of analyzed datasets (i.e. in the datasets of age- matched WT cells cultured with *tor1Δ* mutant cells cultured), were performed using PD2.4 as described in Materials and Methods. The 2-fold increase in the ratio "protein abundance of tor1Δ /protein abundance of WT" represents the upregulation and lower than 0.5 folds in the ratio represent the downregulation of the protein. These proteins include the following ones: (**A**) Protein subunits of the mitochondrial OXPHOS system whose concentrations are increased, (**B**) one of the protein that are negative regulator of OXPHOS that was

downregulated, **(C)** proteins catalyzing heme synthesis and facilitating heme attachment, **(D)** Proteins involved in the TCA cycle. Data are presented as mean values of 2 independent experiments.

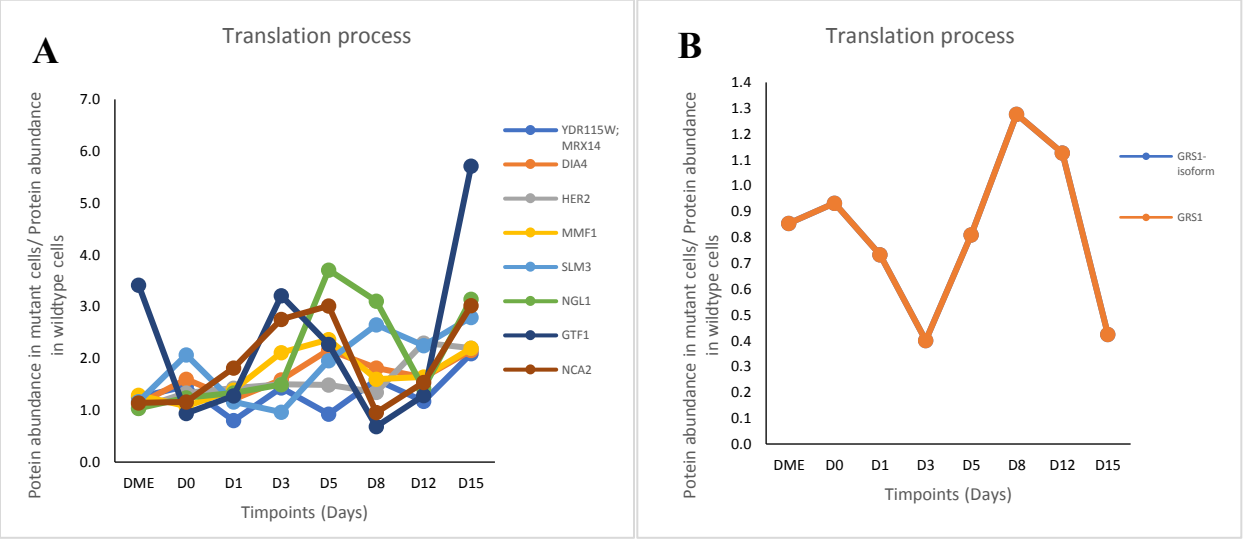

Figure 4.4. The *tor1Δ* mutation alters the abundance of proteins implicated in protein translation in mitochondria. WT and *tor1Δ* mutant cells were cultured in the YEPD (1% yeast extract and 2% peptone) medium initially containing 2% glucose. Cells were recovered on DME, day 0, 1, 3, 5, 8, 12 and 15 of cell culturing were used to purify mitochondria as described in Materials and Methods. Mass spectrometry-based identification and quantitation of mitochondrial proteins recovered from these cells, and the calculation of the relative abundance of mitochondrial proteins in a pair of analyzed datasets (i.e. in the datasets of age- matched WT cells cultured with *tor1Δ* mutant cells cultured), were performed using PD2.4 as described in Materials and Methods. The 2-fold increase in the ratio "protein abundance of tor1Δ /protein abundance of WT" represents the upregulation and lower than 0.5 folds in the ratio represent the downregulation of the protein. These proteins include the following ones: (**A**) Proteins involved in the mitochondrial translation in OXPHOS component, (**B**) proteins involved in translation proteins that are downregulated in day 3. Data are presented as mean values of 2 independent experiments.

4. Conclusion and future studies

This research validates our hypothesis and provides an insight into the mechanism through which TOR1 signaling could control mitochondrial function to affect budding yeast's CLS. The data presented in this thesis support the following conclusions: 1) reduced TOR1 signaling (via *tor1Δ* single-gene-deletion) could enhance the mitochondrial respiration through an increase in the number of some protein complexes involved in the OXPHOS, 2) the up-regulation of OXPHOS complexes proteins involved in ETC occurs primarily by translational regulation, 3) in addition lack of the Tor1 protein controls other aspects of mitochondrial functionality by upregulating proteins involved in mitochondrial fusion and downregulating proteins involved in mitochondrial fission towards stationary growth phase, 4) reduced TOR1 signaling increases the number of mitochondrial membrane proteins involved in lipid synthesis within the mitochondrial membranes, 5) lack of the Tor1 protein increases the number of proteins implicated in protein folding and refolding within mitochondria, and 6) reduced TOR1 signaling decreases the number of proteins involved in ROS production and increase the number of proteins assisting in ROS detoxification during stationary growth phase, thereby limiting the ROS-inflicted oxidative damage to mitochondrial macromolecules (i.e., DNA, proteins and lipids).

The data shows that TOR-dependent alters the function of several mitochondrial proteins under the non-caloric restriction that is crucial in the post-diauxic stationary growth phases that subsequently impact late stationary-phase survival and extend CLS. The response of TOR1 mutation on mitochondrial proteins in yeast CLS is still ongoing research since there are many unknown functions of many identified proteins that were upregulated in the early and late stationary phase.

Taking this research for future research would be interesting to investigate how mutating SCH9 would regulate the mitochondrial proteome for longevity extension by non-caloric restriction in chronological aging yeast. In addition, TOR and PKH1/2 accelerate aging by activating pro-aging protein kinase Sch9. Therefore, inhibiting the PKH1/2 or Sch9 protein kinase can extend CLS and provide a mechanism in mitochondrial proteome changes.

REFERENCES

1. Thermo Proteome Discoverer User Guide. Version 2.4. ThermoFisher Scientific, 2019.
2. López-Otín, C., Blasco, M. A., Partridge, L., Serrano, M., & Kroemer, G. (2013). The hallmarks of aging. Cell, 153(6), 1194–1217. https://doi.org/10.1016/j.cell.2013.05.039
3. Arlia-Ciommo, A., A. Leonov. A. Piano, V. Svistkova, V.I. Titorenko. (2014). Cell-autonomous mechanisms of chronological aging in the yeast Saccharomyces cerevisiae. Microb. Cell. 1:163-178.
4. Fontana, L., L. Partridge, V.D. Longo. (2010). Extending healthy life span-from yeast to humans. Science. 328:321-326.
5. Longo, V.D., G.S. Shadel, M. Kaeberlein, B. Kennedy. (2012). Replicative and chronological aging in Saccharomyces cerevisiae. Cell. 16:18-31.
6. Lutchman, V., P. Dakik, M. McAuley, B. Cortes, G. Ferraye, L. Gontmacher, D. Graziano, F.Z. Moukhariq, E. Simard, V.I. Titorenko. (2016). Six plant extracts delay yeast chronological aging through different signaling pathways. Oncotarget. 32:50845-50863.
7. Bitto, A., Wang, A. M., Bennett, C. F., & Kaeberlein, M. (2015). Biochemical Genetic Pathways that Modulate Aging in Multiple Species. Cold Spring Harbor perspectives in medicine, 5(11), a025114. https://doi.org/10.1101/cshperspect.a025114
8. Swinnen E, Ghillebert R, Wilms T, Winderickx J. Molecular mechanisms linking the evolutionary conserved TORC1-Sch9 nutrient signalling branch to lifespan regulation in Saccharomyces cerevisiae. FEMS Yeast Res. 2014 Feb;14(1):17-32. doi: 10.1111/1567-1364.12097. Epub 2013 Oct 11. PMID: 24102693.
9. Kapahi, P., Chen, D., Rogers, A. N., Katewa, S. D., Li, P. W., Thomas, E. L., & Kockel, L. (2010). With TOR, less is more: a key role for the conserved nutrient-sensing TOR pathway in aging. Cell metabolism, 11(6), 453–465. https://doi.org/10.1016/j.cmet.2010.05.001
10. Eltschinger S, Loewith R. TOR Complexes and the Maintenance of Cellular Homeostasis. Trends Cell Biol. 2016 Feb;26(2):148-159. doi: 10.1016/j.tcb.2015.10.003. Epub 2015 Nov 4. PMID: 26546292.
11. Blenis J. TOR, the Gateway to Cellular Metabolism, Cell Growth, and Disease. Cell. 2017 Sep 21;171(1):10-13. doi: 10.1016/j.cell.2017.08.019. Epub 2017 Sep 6. PMID: 28888322.

12. Brunkard JO. Exaptive Evolution of Target of Rapamycin Signaling in Multicellular Eukaryotes. Dev Cell. 2020 Jul 20;54(2):142-155. doi: 10.1016/j.devcel.2020.06.022. Epub 2020 Jul 9. PMID: 32649861; PMCID: PMC7346820.
13. Kennedy, B. K., & Lamming, D. W. (2016). The Mechanistic Target of Rapamycin: The Grand ConducTOR of Metabolism and Aging. Cell metabolism, 23(6), 990–1003. https://doi.org/10.1016/j.cmet.2016.05.009
14. Evans DS, Kapahi P, Hsueh WC, Kockel L. TOR signaling never gets old: aging, longevity and TORC1 activity. Ageing Res Rev. 2011 Apr;10(2):225-37. doi: 10.1016/j.arr.2010.04.001. Epub 2010 Apr 10. PMID: 20385253; PMCID: PMC2943975.
15. Carl Malina, Christer Larsson, Jens Nielsen, Yeast mitochondria: an overview of mitochondrial biology and the potential of mitochondrial systems biology, FEMS Yeast Research, Volume 18, Issue 5, August 2018, foy040, https://doi.org/10.1093/femsyr/foy040
16. de la Cruz López KG, Toledo Guzmán ME, Sánchez EO, García Carrancá A. mTORC1 as a Regulator of Mitochondrial Functions and a Therapeutic Target in Cancer. Front Oncol. 2019 Dec 13;9:1373. doi: 10.3389/fonc.2019.01373. PMID: 31921637; PMCID: PMC6923780.
17. Bonawitz ND, Chatenay-Lapointe M, Pan Y, Shadel GS. Reduced TOR signaling extends chronological life span via increased respiration and upregulation of mitochondrial gene expression. Cell Metab. 2007 Apr;5(4):265-77. doi: 10.1016/j.cmet.2007.02.009. PMID: 17403371; PMCID: PMC3460550.
18. Pan, Y., & Shadel, G. S. (2009). Extension of chronological life span by reduced TOR signaling requires down-regulation of Sch9p and involves increased mitochondrial OXPHOS complex density. Aging, 1(1), 131–145. https://doi.org/10.18632/aging.100016
19. Pan Y, Schroeder EA, Ocampo A, Barrientos A, Shadel GS. Regulation of yeast chronological life span by TORC1 via adaptive mitochondrial ROS signaling. Cell Metab. 2011 Jun 8;13(6):668-78. doi: 10.1016/j.cmet.2011.03.018. PMID: 21641548; PMCID: PMC3110654.
20. Ruetenik A, Barrientos A. Dietary restriction, mitochondrial function and aging: from yeast to humans. Biochim Biophys Acta. 2015 Nov;1847(11):1434-47. doi:

10.1016/j.bbabio.2015.05.005. Epub 2015 May 12. PMID: 25979234; PMCID: PMC4575837.

21. Beach A, Leonov A, Arlia-Ciommo A, Svistkova V, Lutchman V, Titorenko VI. Mechanisms by which different functional states of mitochondria define yeast longevity. Int J Mol Sci. 2015 Mar 11;16(3):5528-54. doi: 10.3390/ijms16035528. PMID: 25768339; PMCID: PMC4394491.
22. Medkour Y, Dakik P, McAuley M, Mohammad K, Mitrofanova D, Titorenko VI. Mechanisms Underlying the Essential Role of Mitochondrial Membrane Lipids in Yeast Chronological Aging. Oxid Med Cell Longev. 2017; 2017:2916985. doi: 10.1155/2017/2916985. Epub 2017 May 16. PMID: 28593023; PMCID: PMC5448074.
23. Dakik, P., Medkour, Y., Mohammad, K., & Titorenko, V. I. (2019). Mechanisms Through Which Some Mitochondria-Generated Metabolites Act as Second Messengers That Are Essential Contributors to the Aging Process in Eukaryotes Across Phyla. Frontiers in physiology, 10, 461. https://doi.org/10.3389/fphys.2019.00461
24. Kaeberlein, M. (2010). Lessons on longevity from budding yeast. Nature. 464:513-519.
25. van der Bliek AM, Sedensky MM, Morgan PG. Cell Biology of the Mitochondrion. Genetics. 2017 Nov;207(3):843-871. doi: 10.1534/genetics.117.300262. Erratum in: Genetics. 2018 Apr;208(4):1673. PMID: 29097398; PMCID: PMC5676242.
26. Chandel, N. (2015). Evolution of Mitochondria as Signaling Organelles. Cell Metabolism, 22(2), 204-206. doi: 10.1016/j.cmet.2015.05.013

6. Appendix

Table S1: Mitochondrial fusion

Accession	Description	Gene Symbol	DME	D0	D1	D3	D5	D8	D12	D15
P32266	Dynamin-like GTPase MGM1, mitochondrial [OS=Saccharomyces cerevisiae S288C]	MGM1	0.967	0.853	0.903	1.859	1.730	0.894	1.554	3.053
P38297	Mitofusin FZO1 [OS=Saccharomyces cerevisiae S288C]	FZO1	0.881	1.430	1.623	2.229	2.857	2.527	2.747	3.187
Q03327	Mitochondrial fusion and transport protein Ugo1 [OS=Saccharomyces cerevisiae S288C]	UGO1	1.093	0.945	2.053	2.371	2.072	1.602	1.890	3.821

Table S2: Mitochondrial fission

Accession	Description	Gene Symbol	DME	D0	D1	D3	D5	D8	D12	D15
P54861	Dynamin-related protein DNM1 [OS=Saccharomyces cerevisiae S288C]	DNM1	18.288	0.785	3.299	0.142	0.657	1.392	0.334	0.294

Table S3: Mitochondrial protein folding and chaperone

Accession	Description	Gene Symbol	DME	D0	D1	D3	D5	D8	D12	D15
P39987	Heat shock protein SSC3, mitochondrial [OS=Saccharomyces cerevisiae S288C]	ECM10	1.142	3.762	2.043	2.130	2.640	3.440	6.935	2.035
P21560	Protein CBP3, mitochondrial [OS=Saccharomyces cerevisiae S288C]	CBP3	2.722	0.610	1.014	1.358	1.961	0.913	0.815	2.178
P38910	10 kDa heat shock protein, mitochondrial [OS=Saccharomyces cerevisiae S288C]	HSP10	1.285	1.020	1.263	1.792	1.678	1.168	1.345	2.238
P33416	Heat shock protein 78, mitochondrial [OS=Saccharomyces cerevisiae S288C]	HSP78	1.090	1.830	1.403	1.847	1.980	1.694	1.927	2.718
P40961	prohibitin-1 [OS=Saccharomyces cerevisiae S288C]	PHB1	1.042	1.060	1.616	2.270	1.990	1.182	0.990	3.391
P25573	Mitochondrial inner membrane i-AAA protease supercomplex subunit MGR1 [OS=Saccharomyces cerevisiae S288C]	MGR1	1.147	1.192	1.897	2.039	2.493	1.524	1.698	2.703

Table S4: Mitochondrial organisation

Accession	Description	Gene Symbol	DME	D0	D1	D3	D5	D8	D12	D15
P35691	Translationally controlled tumor protein homolog [OS=Saccharomyces cerevisiae S288C]	TMA19	1.293	0.714	0.963	1.136	2.446	2.586	0.470	0.438
P50087	MICOS subunit MIC26 [OS=Saccharomyces cerevisiae S288C]	MOS2; MIC26	1.119	0.830	1.474	1.692	1.821	0.967	1.107	2.101
P38880	Mitochondrial distribution and morphology protein 31 [OS=Saccharomyces cerevisiae S288C]	MDM31	0.891	1.067	2.044	0.997	1.026	1.532	2.222	2.354
P50945	MICOS complex subunit MIC27 [OS=Saccharomyces cerevisiae S288C]	AIM37; MIC27	1.217	0.854	1.542	1.718	1.912	0.916	0.988	3.150
Q12171	Mitochondrial distribution and morphology protein 32 [OS=Saccharomyces cerevisiae S288C]	MDM32	0.772	1.711	1.016	1.935	4.038	3.499	2.962	8.508

Table S5: Protein and ion transport

Accession	Description	Gene Symbol	DME	D0	D1	D3	D5	D8	D12	D15
P53969	Sorting assembly machinery 50 kDa subunit [OS=Saccharomyces cerevisiae S288C]	SAM50	1.211	1.032	1.135	1.715	1.898	1.547	0.936	2.218
P36147	Presequence translocated-associated motor subunit pam17, mitochondrial [OS=Saccharomyces cerevisiae S288C]	PAM17	1.424	1.152	1.941	1.497	2.435	1.096	1.068	2.316
P04710	ADP,ATP carrier protein 1 [OS=Saccharomyces cerevisiae S288C]	AAC1	1.386	0.982	1.322	1.150	1.332	0.869	1.428	2.438
P32897	Mitochondrial import inner membrane translocase subunit tim23 [OS=Saccharomyces cerevisiae S288C]	TIM23	1.117	0.870	1.646	2.816	1.945	1.062	0.953	2.454
P32331	Carrier protein YMC1, mitochondrial [OS=Saccharomyces cerevisiae S288C]	YMC1	0.975	1.185	1.513	1.367	1.625	0.995	1.343	2.495
Q12328	Mitochondrial import inner membrane translocase subunit TIM22 [OS=Saccharomyces cerevisiae S288C]	TIM22	1.164	0.842	1.196	1.923	1.815	0.914	1.525	2.567
Q12482	Mitochondrial aspartate-glutamate transporter AGC1 [OS=Saccharomyces cerevisiae S288C]	AGC1	1.321	2.059	1.203	0.981	0.854	0.794	1.223	3.640
P23500	Mitochondrial RNA-splicing protein MRS4 [OS=Saccharomyces cerevisiae S288C]	MRS4	1.734	1.279	1.390	1.046	2.116	2.073	2.094	3.665
P47045	mitochondrial import inner membrane translocase	TIM54	1.211	1.002	1.796	3.584	3.311	1.743	1.584	4.110

	subunit TIM54 [OS=Saccharomyces cerevisiae S288C]									
P23644	Mitochondrial import receptor subunit TOM40 [OS=Saccharomyces cerevisiae S288C]	TOM40	1.020	0.370	2.289	2.629	3.323	1.006	0.773	4.246
P50110	Sorting assembly machinery 37 kDa subunit [OS=Saccharomyces cerevisiae S288C]	SAM37	1.299	1.141	1.448	2.209	2.471	2.037	1.196	4.974
P39986	Manganese-transporting ATPase 1 [OS=Saccharomyces cerevisiae S288C]	SPF1	1.008	0.565	1.777	13.990	10.990	0.921	4.732	5.609
P38825	Protein TOM71 [OS=Saccharomyces cerevisiae S288C]	TOM71	0.945	1.296	1.607	1.809	2.084	1.975	2.485	2.268

Table S6: Carbohydrate metabolism

Accession	Description	Gene Symbol	DME	D0	D1	D3	D5	D8	D12	D15
P04807	Hexokinase-2 [OS=Saccharomyces cerevisiae S288C]	HXK2	1.118	1.041	1.759	1.376	1.521	1.821	0.494	0.336
P00560	Phosphoglycerate kinase [OS=Saccharomyces cerevisiae S288C]	PGK1	1.146	1.204	0.686	0.631	0.753	1.208	0.615	0.378
P04806	Hexokinase-1 [OS=Saccharomyces cerevisiae S288C]	HXK1	1.195	1.005	0.948	0.611	0.540	0.923	0.693	0.390
P00950	Phosphoglycerate mutase 1 [OS=Saccharomyces cerevisiae S288C]	GPM1	1.267	0.664	0.744	0.759	0.671	1.166	0.829	0.398
P00925	Enolase 2 [OS=Saccharomyces cerevisiae S288C]	ENO2	1.223	0.753	1.202	1.028	0.664	1.760	0.660	0.478
P12709	glucose-6-phosphate isomerase [OS=Saccharomyces cerevisiae S288C]	PGI1	0.826	1.226	0.871	0.712	0.992	1.773	0.720	0.492

Table S7: ROS

Accession	Description	Gene Symbol	DME	D0	D1	D3	D5	D8	D12	D15
P00445	Superoxide dismutase [Cu-Zn] [OS=Saccharomyces cerevisiae S288C]	SOD1	1.604	0.831	0.662	1.710	1.116	2.379	4.462	2.017
Q12207	Non-classical export protein 2 [OS=Saccharomyces cerevisiae S288C]	NCE102	2.165	1.709	6.680	7.074	9.377	3.889	1.654	2.188
P36060	NADH-cytochrome b5 reductase 2 [OS=Saccharomyces cerevisiae S288C]	MCR1	1.600	1.110	1.069	1.438	1.515	1.833	1.948	2.203
P38816	thioredoxin reductase 2, mitochondrial [OS=Saccharomyces cerevisiae S288C]	TRR2	1.154	1.174	1.389	2.182	1.919	2.065	1.958	2.487
P00431	cytochrome c peroxidase, mitochondrial [OS=Saccharomyces cerevisiae S288C]	CCP1	1.336	0.659	0.744	1.388	1.824	1.255	2.458	2.555
P17695	Glutaredoxin-2, mitochondrial [OS=Saccharomyces cerevisiae S288C]	GRX2	1.212	0.851	1.388	1.519	1.694	1.565	1.212	2.618
P25372	Thioredoxin-3, mitochondrial [OS=Saccharomyces cerevisiae S288C]	TRX3	1.456	1.253	1.325	1.940	3.124	2.377	2.932	3.091
P38969	Pentamidine resistance factor, mitochondrial [OS=Saccharomyces cerevisiae S288C]	PNT1	1.186	0.952	1.704	1.984	1.870	1.112	0.962	3.315
Q02784	Monothiol glutaredoxin-5, mitochondrial [OS=Saccharomyces cerevisiae S288C]	GRX5	0.783	0.943	0.691	1.236	1.488	1.078	1.323	3.471

P29509	thioredoxin reductase 1 [OS=Saccharomyces cerevisiae S288C]	TRR1	1.007	0.900	1.380	3.506	1.761	2.058	1.286	4.276

Table S8: Lipid metabolism

Accession	Description	Gene Symbol	DME	D0	D1	D3	D5	D8	D12	D15
Q12283	Malonyl CoA-acyl carrier protein transacylase, mitochondrial [OS=Saccharomyces cerevisiae S288C]	MCT1	1.204	1.049	1.564	2.397	2.252	1.626	1.516	2.078
P38812	Phosphatidylglycerophosphatase GEP4, mitochondrial [OS=Saccharomyces cerevisiae S288C]	GEP4	0.853	0.874	1.387	2.238	2.732	1.307	1.511	2.622
Q02883	N-acyl-phosphatidylethanolamine-hydrolyzing phospholipase D, mitochondrial [OS=Saccharomyces cerevisiae S288C]	FMP30	1.185	1.305	2.049	3.144	2.070	1.296	2.351	2.826
P35731	3-oxoacyl-[acyl-carrier-protein] reductase [OS=Saccharomyces cerevisiae S288C]	OAR1	1.661	1.122	1.108	5.585	5.030	0.877	1.094	3.398
P46998	mitochondrial membrane protein FMP33 [OS=Saccharomyces cerevisiae S288C]	FMP33	1.290	1.151	2.201	1.835	2.624	1.571	2.140	4.726

Table S9: OXPHOS and ETC

Accession	Description	Gene Symbol	DME	D0	D1	D3	D5	D8	D12	D15
P37299	cytochrome b-c1 complex subunit 10 [OS=Saccharomyces cerevisiae S288C]	QCR10	1.131	1.318	1.071	1.454	1.478	1.181	1.592	2.007
P08525	Cytochrome b-c1 complex subunit 8 [OS=Saccharomyces cerevisiae S288C]	QCR8	1.591	1.198	1.281	1.962	1.692	1.285	1.495	2.518
P08067	cytochrome b-c1 complex subunit Rieske, mitochondrial [OS=Saccharomyces cerevisiae S288C]	RIP1	1.166	0.974	1.575	1.599	1.296	1.269	1.359	2.577
P10174	cytochrome c oxidase subunit 7 [OS=Saccharomyces cerevisiae S288C]	COX7	1.073	1.117	2.147	4.077	1.530	1.867	2.774	2.142
P00401	Cytochrome c oxidase subunit 1 [OS=Saccharomyces cerevisiae S288C]	COX1	0.873	1.153	0.812	0.609	2.979	0.827	2.907	2.336
Q2V2P9	Uncharacterized protein YDR119W-A [OS=Saccharomyces cerevisiae S288C]	COX26	1.647	1.025	1.465	2.843	1.448	0.918	1.062	2.397
P19516	Cytochrome c oxidase assembly protein COX11, mitochondrial [OS=Saccharomyces cerevisiae S288C]	COX11	1.196	1.152	2.269	1.607	1.201	1.169	1.280	2.662
P81449	ATP synthase subunit e, mitochondrial [OS=Saccharomyces cerevisiae S288C]	TIM11	0.926	1.443	1.488	1.720	1.827	0.939	1.247	2.357
Q12233	ATP synthase subunit g, mitochondrial [OS=Saccharomyces cerevisiae S288C]	ATP20	1.395	1.235	1.531	2.043	2.139	1.052	0.972	2.903

P00427	Cytochrome c oxidase subunit 6, mitochondrial [OS=Saccharomyces cerevisiae S288C]	COX6	1.070	0.932	0.937	0.846	0.900	0.531	0.683	3.178
P40452	Cytochrome c oxidase assembly factor 1 [OS=Saccharomyces cerevisiae S288C]	COA1	1.348	1.007	1.385	0.806	2.024	0.965	1.042	2.450
P01097	ATPase inhibitor, mitochondrial [OS=Saccharomyces cerevisiae S288C]	INH1	1.272	0.663	0.705	1.127	0.439	1.561	1.810	0.474

Table S10: Heme synthesis

Accession	Description	Gene Symbol	DME	D0	D1	D3	D5	D8	D12	D15
P16622	Ferrochelatase, mitochondrial [OS=Saccharomyces cerevisiae S288C]	HEM15	1.244	0.926	1.782	2.256	2.485	1.843	0.936	2.441
P00045	Cytochrome c iso-2 [OS=Saccharomyces cerevisiae S288C]	CYC7	0.934	1.117	1.227	1.649	2.692	2.801	4.010	2.310
Q00873	cytochrome c1 heme lyase [OS=Saccharomyces cerevisiae S288C]	CYT2	1.103	1.633	1.431	1.617	1.610	1.899	2.085	2.506

Table S11: Tricarboxylic acid

Accession	Description	Gene Symbol	DME	D0	D1	D3	D5	D8	D12	D15
P38152	Tricarboxylate transport protein [OS=Saccharomyces cerevisiae S288C]	CTP1	0.958	1.165	1.542	1.264	1.450	1.516	1.290	2.142
Q06236	Mitochondrial inner membrane protein SHH4 [OS=Saccharomyces cerevisiae S288C]	SHH4	0.841	1.864	1.839	1.697	2.551	1.882	3.573	5.149

Table S12: Translation process

Accession	Description	Gene Symbol	DME	D0	D1	D3	D5	D8	D12	D15
Q04598	54S ribosomal protein L34, mitochondrial [OS=Saccharomyces cerevisiae S288C]	YDR115W; MRX14	1.256	1.467	0.802	1.436	0.929	1.589	1.176	2.093
P38705	Serine--tRNA ligase, mitochondrial [OS=Saccharomyces cerevisiae S288C]	DIA4	1.118	1.601	1.213	1.591	2.166	1.817	1.631	2.157
Q03557	Glutamyl-tRNA(Gln) amidotransferase subunit A, mitochondrial [OS=Saccharomyces cerevisiae S288C]	HER2	1.037	1.333	1.430	1.501	1.488	1.345	2.301	2.201
P40185	Protein mmf1, mitochondrial [OS=Saccharomyces cerevisiae S288C]	MMF1	1.289	1.078	1.390	2.110	2.365	1.602	1.641	2.202
Q12093	Mitochondrial tRNA-specific 2-thiouridylase 1 [OS=Saccharomyces cerevisiae S288C]	SLM3	1.169	2.067	1.162	0.964	1.957	2.650	2.248	2.795
Q08213	RNA exonuclease NGL1 [OS=Saccharomyces cerevisiae S288C]	NGL1	1.038	1.242	1.333	1.493	3.709	3.109	1.421	3.147

P53260	Glutamyl-tRNA(Gln) amidotransferase subunit F, mitochondrial [OS=Saccharomyces cerevisiae S288C]	GTF1	3.419	0.942	1.277	3.214	2.273	0.687	1.286	5.715
Q12374	Nuclear control of ATPase protein 2 [OS=Saccharomyces cerevisiae S288C]	NCA2	1.143	1.159	1.814	2.753	3.017	0.956	1.542	3.022

Table S13: Translation process

Accession	Description	Gene Symbol	DME	D0	D1	D3	D5	D8	D12	D15
P38088-2	Isoform Cytoplasmic of Glycine--tRNA ligase 1, mitochondrial [OS=Saccharomyces cerevisiae S288C]	GRS1	0.854	0.932	0.733	0.401	0.809	1.277	1.127	0.425
P38088	Glycine--tRNA ligase 1, mitochondrial [OS=Saccharomyces cerevisiae S288C]	GRS1	0.854	0.932	0.733	0.401	0.809	1.277	1.127	0.425